Guard Cell Starch Degradation Yields Glucose for Rapid Stomatal Opening in Arabidopsis

Journal Article

Author(s):
Flütsch, Sabrina [ID]; Wang, Yizhou; Takemiya, Atsushi; Vialet-Chabrand, Silvere R. M.; Klejchová, Martina; Nigro, Arianna; Hills, Adrian; Lawson, Tracy; Blatt, Michael R.; Santelia, Diana

Guard Cell Starch Degradation Yields Glucose for Rapid Stomatal Opening in Arabidopsis[CC-BY]

Sabrina Flütsch,[a,b] Yizhou Wang,[c,1] Atsushi Takemiya,[d] Silvere R. M. Vialet-Chabrand,[e] Martina Klejchová,[c] Arianna Nigro,[b,2] Adrian Hills,[c] Tracy Lawson,[e] Michael R. Blatt,[c] and Diana Santelia[a,b,3]

[a] Institute of Integrative Biology, Eidgenössische Technische Hochschule (ETH) Zürich, CH–8092 Zürich, Switzerland

[b] Department of Plant and Microbial Biology, University of Zürich, CH-8008, Zürich, Switzerland

[c] Laboratory of Plant Physiology and Biophysics, University of Glasgow, Glasgow G12 8QQ, United Kingdom

[d] Department of Biology, Graduate School of Sciences and Technology for Innovation, Yamaguchi University, 753–8512 Yamaguchi, Japan

[e] School of Life Sciences, University of Essex, Colchester, CO4 3SQ, United Kingdom

ORCID IDs: 0000-0001-7020-6520 (S.F.); 0000-0002-2188-383X (Y.W.); 0000-0003-2642-6758 (A.T.); 0000-0002-2105-2825 (S.R.M.V.-C.); 0000-0002-1446-0791 (M.K.); 0000-0003-3928-3469 (A.N.); 0000-0002-4705-0756 (A.H.); 0000-0002-4073-7221 (T.L.); 0000-0003-1361-4645 (M.R.B.); 0000-0001-9686-1216 (D.S.)

Starch in Arabidopsis (*Arabidopsis thaliana*) guard cells is rapidly degraded at the start of the day by the glucan hydrolases α-AMYLASE3 (AMY3) and β-AMYLASE1 (BAM1) to promote stomatal opening. This process is activated via phototropin-mediated blue light signaling downstream of the plasma membrane H^+-ATPase. It remains unknown how guard cell starch degradation integrates with light-regulated membrane transport processes in the fine control of stomatal opening kinetics. We report that H^+, K^+, and Cl^- transport across the guard cell plasma membrane is unaltered in the *amy3 bam1* mutant, suggesting that starch degradation products do not directly affect the capacity to transport ions. Enzymatic quantification revealed that after 30 min of blue light illumination, *amy3 bam1* guard cells had similar malate levels as the wild type, but had dramatically altered sugar homeostasis, with almost undetectable amounts of Glc. Thus, Glc, not malate, is the major starch-derived metabolite in Arabidopsis guard cells. We further show that impaired starch degradation in the *amy3 bam1* mutant resulted in an increase in the time constant for opening of 40 min. We conclude that rapid starch degradation at dawn is required to maintain the cytoplasmic sugar pool, clearly needed for fast stomatal opening. The conversion and exchange of metabolites between subcellular compartments therefore coordinates the energetic and metabolic status of the cell with membrane ion transport.

INTRODUCTION

Stomata are microscopic pores in the plant epidermis bounded by a pair of guard cells. The appearance of stomata was a major evolutionary innovation for the transition of plants to life on land (Hetherington and Woodward, 2003; Berry et al., 2010); they interrupt the impermeable waxy cuticle and open to facilitate CO_2 diffusion into the leaves for photosynthesis (CO_2 assimilation, A). This process, however, also allows water to diffuse out of the leaf through the evapotranspiration stream, risking desiccation. The capacity of stomata to enable CO_2 uptake or water loss is known as stomatal conductance (g_s), and measured as a mole flux per unit area (mol m^{-2} s^{-1}). To optimize daytime water use efficiency (WUE; amount of carbon fixed per unit water loss,

A/evapotranspiration) and survive the harsh terrestrial environment, plants have evolved the capacity to actively control the stomatal pore aperture and change g_s in response to fluctuating environmental conditions (Haworth et al., 2011). Plants generally open their stomata (increase in g_s) in response to light and low CO_2 concentrations, while they close them (decrease in g_s) in darkness, in response to high CO_2 concentrations, and under adverse environmental conditions (Murata et al., 2015).

In the steady state, changes in A are often strongly associated with g_s dynamics, leading to a near-optimal balance of carbon gain and water loss (Wong et al., 1979). In fluctuating environments, however, stomatal responses to changing conditions, especially light and temperature, are generally slower than photosynthetic responses (Lawson and Blatt, 2014; Lawson and Vialet-Chabrand, 2019). For example, upon changes in photosynthetic photon flux density during sun/shade flecks caused by passing clouds or overlapping leaves in a canopy, A adapts quickly by reaching a new steady state within several tens of seconds to minutes, whereas changes in g_s can take minutes to hours (Barradas and Jones, 1996; Ooba and Takahashi, 2003; Vico et al., 2011; McAusland et al., 2016; Vialet-Chabrand et al., 2016; Lawson and Vialet-Chabrand, 2019). Despite considerable variation in the magnitude and time scales of opening and closing responses across species and environmental conditions (Barradas and Jones, 1996; Vico et al., 2011; McAusland et al., 2016; Qu et al., 2016),

IN A NUTSHELL

Background: Stomatal opening is driven by the blue light-activated H⁺-ATPase (AHA1) at the guard cell plasma membrane, which hyperpolarizes the plasma membrane causing the intake of potassium (K^+), chloride (Cl^-), malate^{2-} (Mal) and nitrate (NO_3^-), resulting in increased cell turgor and stomatal aperture. In parallel to the activation of membrane ion transport, guard cell starch is rapidly degraded upon illumination after dawn through the coordinated activity of the glucan hydrolases α-amylase 3 (AMY3) and β-amylase 1 (BAM1) to promote stomatal opening. Arabidopsis plants simultaneously lacking BAM1 and AMY3 open their stomata more slowly and to a lesser extent. Guard cell starch is supposed to be converted into Mal. As protons (H+) are produced during this conversion, reduced Mal availibility and H⁺ load might directly alter the capacity of membrane ion transport during stomatal opening, potentially explaining the reduced stomatal opening response of *amy3 bam1* plants.

Question: What mechanism underlies the delayed light-induced stomatal opening in mutants deficient in AMY3 and BAM1?

Findings: We show that transport of H⁺, K⁺ and Cl⁻ ions across the guard cell plasma membrane was unaffected in *amy3 bam1* mutants, demonstrating that starch degradation does not directly alter the ability to transport ions during stomatal opening. Enzymatic assays revaled that Mal content in wild-type and *amy3 bam1* guard cells under blue light was similar, suggesting that starch mobilization does not directly result in Mal production, likely explaining the absence of alterations in membrane ion transport in the *amy3 bam1* mutant. Surprisingly, *amy3 bam1* guard cells had dramatically altered sugar homeostasis during blue light-induced stomatal opening with substantially reduced Glc amounts. We conclude that Glc is the major guard cell starch derived metabolite in Arabidopsis and that the reduced and slow stomatal opening response of *amy3 bam1* plants results from insufficient availability of carbon within guard cells.

Next steps: Future work should examine the fate of starch-derived Glc in guard cells during stomatal opening.

stomatal delays to light fluctuations have a well-documented impact on the economics of leaf gas exchange, with important implications in terms of *A* and transpiration and, hence, leaf WUE (Naumburg et al., 2001; Lawson and Blatt, 2014; Vialet-Chabrand et al., 2017b; Lawson and Vialet-Chabrand, 2019).

Many studies have explored stomatal anatomy, size, and density as strategies for increasing or decreasing g_s, based on the assumption that high densities of small stomata can alter aperture faster than fewer, larger stomata (Hetherington and Woodward, 2003; Franks and Beerling, 2009; Drake et al., 2013; Raven, 2014). These approaches have often met with limited success. Modifications of stomatal density that result in gain in *A* through increases in g_s can occur at the expense of WUE (Tanaka et al., 2013). Furthermore, manipulation of physical attributes may be counterbalanced by unpredicted modifications in function (Büssis et al., 2006). This holds true especially for species with elliptical (or kidney-shaped) guard cells, such as Arabidopsis spp and many crop plants, in which differences in g_s responses cannot simply be explained by the size of stomata (Elliott-Kingston et al., 2016; McAusland et al., 2016).

A less obvious and a relatively unexplored approach exploits stomatal movement kinetics to facilitate coordinated g_s responses with mesophyll demands for CO_2 (Vialet-Chabrand et al., 2017a). Modeled synchronous behavior in g_s and *A* in *Phaseolus vulgaris* subjected to dynamic light has been shown to theoretically increase WUE by 20% (Lawson and Blatt, 2014; Lawson and Vialet-Chabrand, 2019). Furthermore, optogenetic manipulation of stomatal kinetics by expression of the synthetic, light-gated potassium (K⁺) channel BLINK1 in Arabidopsis guard cells demonstrated a 2-fold enhancement of WUE (Papanatsiou et al., 2019). These gains, in turn, would substantially boost plant growth and yield. A current limitation of this strategy is that a full

mechanistic understanding of the molecular components determining g_s kinetics is still lacking.

Stomatal opening is powered by the blue light (BL)-activated H⁺-ATPase (AHA1) at the guard cell plasma membrane (PM), which hyperpolarizes the membrane potential by pumping H⁺ out of the guard cells (Assmann et al., 1985; Shimazaki et al., 1986). The hyperpolarization drives K⁺ uptake through the inward-rectifying K⁺ channels with accumulation of malate^{2-} (Mal), chloride (Cl⁻), and nitrate, driving changes in cell turgor and stomatal aperture (Inoue and Kinoshita, 2017; Jezek and Blatt, 2017). BL simultaneously inhibits the S-type anion channel activities via CONVERGENCE OF BL AND CO_2 protein kinases to support stomatal opening (Marten et al., 2007; Hiyama et al., 2017).

In parallel to the activation of membrane ion transport, starch in guard cell chloroplasts is degraded within the first hour of light, contributing to a rapid increase in stomatal aperture (Horrer et al., 2016). In the *amy3 bam1* double mutant, which lacks the glucan hydrolases β-amylase1 (BAM1) and α-amylase3 (AMY3) needed to break down this starch, stomata open more slowly and to a lesser extent (Horrer et al., 2016). Early studies hypothesized that carbon skeletons derived from starch degradation are used to synthesize Mal. This hypothesis is based on experiments linking changes in guard cell protoplast (GCP) volume to changes in Mal content (Schnabl, 1980a; Schnabl et al., 1982) as well as loss of starch in guard cells in the light (Lloyd, 1908; Outlaw and Manchester, 1979).

Interestingly, starch degradation is triggered by low levels of BL through the phototropin-mediated signaling cascade (Tallman and Zeiger, 1988; Horrer et al., 2016). Arabidopsis mutants lacking AHA1 also show defective guard cell starch degradation, indicating a coordinate requirement for the PM H⁺-ATPase (Horrer et al., 2016).

This previously unexpected connection between light-regulated membrane ion transport and guard cell starch metabolism prompted us to investigate how these processes integrate in the fine control of stomatal opening kinetics. We found that H^+, K^+, and Cl^- transport across the guard cell PM is unaltered in the Arabidopsis stomatal starch-degrading mutant *amy3 bam1*, suggesting that starch degradation products do not directly affect the capacity to transport ions. Despite the long-held view that Mal derives from starch degradation, we observed that Mal levels in guard cells of *amy3 bam1* were similar to those of the wild type, whereas Glc levels were greatly reduced. Rapid starch degradation at dawn is therefore very likely required to maintain sugar homeostasis during stomatal opening. By comparing g_s kinetics with guard cell starch dynamics in plants subjected to pulses of light and darkness under common light growth conditions (150 μmol m^{-2} s^{-1}), we further show that the amounts of starch and the ability to promptly break it down upon transition to light are associated with fast stomatal opening kinetics. Impaired guard cell starch degradation in the *amy3 bam1* or *aha1* mutant caused up to 40 min delay to reach 63% of the maximal g_s amplitude compared with the wild type, which was not linked with stomatal size and density. In response to pulses of higher light intensity (400 μmol m^{-2} s^{-1}) or in response to red light (RL; 300 μmol m^{-2} s^{-1}), under which the plant is photosynthesis-saturated, g_s kinetics did not depend on starch degradation. Finally, we provide evidence that fast g_s kinetics under RL are primarily driven by photosynthetic production of Suc in the mesophyll and the import to guard cells, as energized by the PM H^+-ATPase AHA1. Our findings provide insights into the molecular mechanisms determining fast stomatal opening kinetics to light in Arabidopsis, showing that they depend on a tight coordination between membrane ion transport and metabolic rearrangements.

RESULTS

BL-Induced Proton Pumping, K^+ and Cl^- Channel Activities Are Unaltered in *amy3 bam1* Mutants

The major starch-degrading enzyme in Arabidopsis guard cells is BAM1, an exoamylase that attacks the nonreducing end of the glucan chains to release maltose. Upon illumination, BAM1 rapidly mobilizes starch in conjunction with the chloroplastic AMY3, an endoamylase that hydrolyzes α-1,4 bonds within glucan chains. Simultaneous loss of BAM1 and AMY3 in the *amy3 bam1* double mutant leads to elevated guard cell starch levels throughout the diurnal cycle, severely affecting stomatal opening (Horrer et al., 2016). Guard cell starch is thought to be converted to Mal (Raschke and Schnabl, 1978; Schnabl, 1980a). Therefore, we hypothesized that reduced Mal synthesis and H^+ accumulation associated with the inhibition of starch degradation in *amy3 bam1* would suppress H^+-ATPase activity and reduce membrane voltage, and consequently limit the driving force for ion uptake, potentially explaining the defective stomatal opening response of *amy3 bam1* (Blatt, 2016).

To test this hypothesis, we first examined the activity of the H^+-ATPase in GCPs in response to BL illumination (10 μmol m^{-2} s^{-1} BL superimposed to 50 μmol m^{-2} s^{-1} RL). Recordings of H^+ pumping in wild-type GCPs yielded an average H^+ flux of 0.72 nmol h^{-1} μg protein^{-1} (Figures 1A and 1B), which is in line with H^+ fluxes

reported in other studies (Ueno et al., 2005; Hiyama et al., 2017). The H^+ extrusion measured here is also consistent with the H^+-ATPase activity needed to drive solute uptake for stomatal opening for intact guard cells (Wang et al., 2012, 2017), as supported by the estimation of the H^+ extrusion rate presented in Supplemental File 1. To our surprise, GCPs from *amy3 bam1* plants showed similar rates of BL-induced H^+ pumping to those of the wild type (0.68 nmol h^{-1} μg protein^{-1}; Figures 1A and 1B), as well as similar levels of phosphorylation of the H^+-ATPase (Figure 1C; Supplemental Figure 1A). While we did not detect differences in H^+ pumping, *amy3 bam1* plants showed slow g_s kinetics and reduced amplitudes when exposed to the same light conditions (Supplemental Figure 1B). These results indicate a fully functional proton pump, even in the absence of starch degradation.

Next, we recorded K^+ and Cl^- channel currents under voltage clamp from intact guard cells. These methods bring membrane voltage under direct experimental control, thereby separating channel activity from complications of changes in membrane energization. Our voltage-clamp recordings detected no differences in K^+ and Cl^- currents, their activation kinetics, or their conductances between the wild type and *amy3 bam1*, indicating that the mutation did not alter the capacity for K^+ or Cl^- uptake (Figures 1D and 1E).

BL-Induced Guard Cell Starch Degradation Yields Glc

In our current model, Mal in guard cells is postulated to derive mainly from BL-induced starch degradation. This model is based on early publications (Raschke and Schnabl, 1978; Schnabl, 1980a), mostly correlative in nature, and lacks biochemical validation. To assess whether starch is indeed converted to Mal, we quantified Mal by enzymatic methods in wild-type and *amy3 bam1* guard-cell–enriched epidermal peels exposed to BL (75 μmol m^{-2} s^{-1}) for 30 min. Mal levels in peels harvested at the end of the night (EoN) were similar in both genotypes (Figure 2A; Supplemental Table 1). Mal then decreased to a similar extent when isolated peels floating in opening buffer were illuminated with BL (Figure 2A; Supplemental Table 1), presumably as it was further metabolized to energize stomatal opening. However, Mal levels remained unchanged if the peels were kept in the dark for 30 min (Supplemental Figure 2A), indicating that the decrease in Mal was specifically induced by BL illumination. As a control, we measured Mal content in the leaves at the EoN, and found no differences between wild-type and *amy3 bam1* plants (Supplemental Figure 2B). Altogether, these data suggest that Mal is metabolized in guard cells in response to BL, most likely for energy production. Furthermore, starch degradation in Arabidopsis guard cells does not directly result in Mal production, likely explaining why membrane ion transport is unaltered in *amy3 bam1* (Figure 1).

Given that there were no differences in Mal content, we reasoned that degradation of starch might directly influence soluble sugar homeostasis. We therefore quantified Glc, Fru, and Suc in guard-cell–enriched epidermal peels exposed to BL as detailed above. The wild type had substantial amounts of Glc at the EoN and lower quantities of Fru and Suc (Figure 2B; Supplemental Figure 2C; Supplemental Table 2). Fru and Suc then decreased when isolated peels floating in opening buffer were exposed to BL, while Glc levels did not significantly change (Figure 2B;
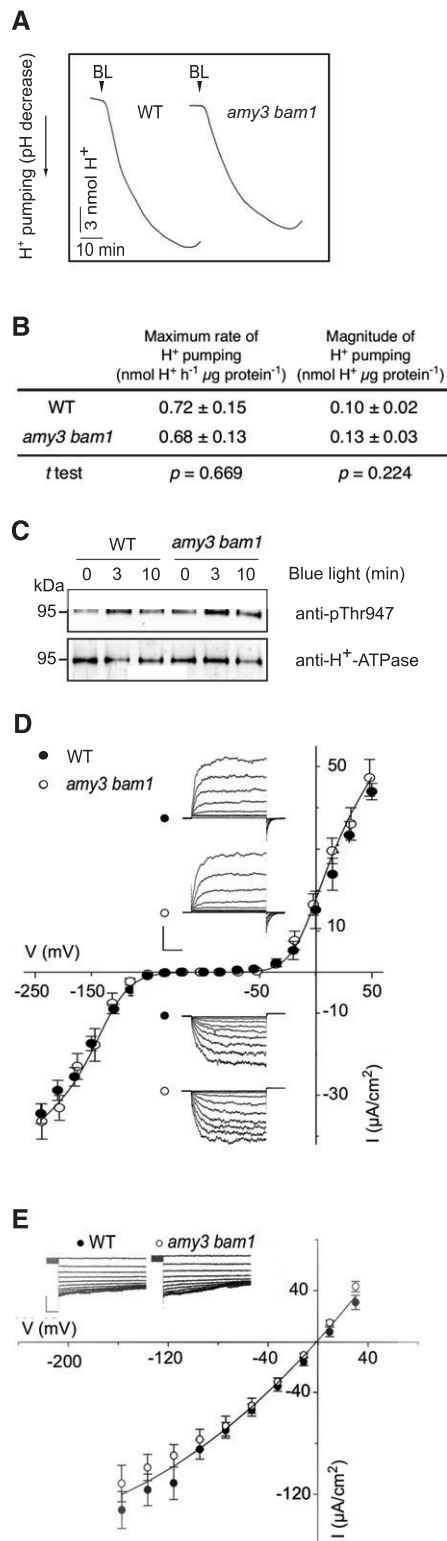
A

B

	Maximum rate of H⁺ pumping (nmol H⁺ h⁻¹ µg protein⁻¹)	Magnitude of H⁺ pumping (nmol H⁺ µg protein⁻¹)
WT	0.72 ± 0.15	0.10 ± 0.02
amy3 bam1	0.68 ± 0.13	0.13 ± 0.03
t test	$p = 0.669$	$p = 0.224$

C

D

E

Figure 1. Membrane Ion Transport in Wild-Type and *amy3 bam1* Guard Cells.

(A) BL-dependent H⁺ pumping in GCPs. GCPs were exposed to RL (50 µmol m⁻² s⁻¹) for 2 h, after which BL (10 µmol m⁻² s⁻¹) was applied for 30

Supplemental Table 2). Notably, *amy3 bam1* guard cells had only half as much Glc as those of the wild type at the EoN (Figure 2B; Supplemental Figure 2C), and almost undetectable amounts after the light treatment (Figure 2B). Fru levels were similar to the wild type, but, surprisingly, *amy3 bam1* guard cells had 3- to 4-fold more Suc than the wild type at the EoN (Figure 2B; Supplemental Figure 2C; Supplemental Table 2). Interestingly, *amy3 bam1* plants contained elevated amounts of Suc at the EoN in the leaves as well, possibly explaining the high Suc content in guard cells, whereas leaf levels of Glc and Fru were similar to the wild type (Supplemental Figure 2D). Suc in guard cells was then depleted in both the wild type and *amy3 bam1* after 30 min of BL illumination (Figure 2B), consistent with the idea that Suc is a substrate for light-induced stomatal opening (Lima et al., 2018; Medeiros et al., 2018). If isolated wild-type guard cells were kept in the dark for 30 min, Glc levels decreased to less than half (Supplemental Figure 2C), suggesting that the sustained levels of Glc in wild-type guard cells under BL result from BL-induced starch degradation. Glc was also partially metabolized in *amy3 bam1* guard cells during dark incubation (Supplemental Figure 2C). Fru levels decreased in wild-type guard cells but not in that of *amy3 bam1* (Supplemental Figure 2C), while Suc remained unchanged during the 30 min of dark incubation (Supplemental Figure 2C). This result further supports the role of Suc as an energy supplier during light-induced stomatal opening. Overall, our findings suggest that under BL, isolated Arabidopsis guard cells release Glc from starch degradation. Thus, the slow and reduced stomatal opening of *amy3 bam1* at the start of the day (Horrer et al., 2016) is a consequence of altered guard cell sugar homeostasis.

Fast Stomatal Opening Kinetics Are Associated with the Rate of Guard Cell Starch Degradation in Arabidopsis Plants Subjected To Alternating Pulses of Light and Darkness

Our electrophysiological and metabolite measurements ruled out a forward impact of starch degradation on membrane ion

min. One representative experiment out of five experiments is shown. WT, wild type.

(B) BL-dependent H⁺ pumping quantification. Values represent means ± SE ($n = 5$).

(C) Immunoblots of BL-dependent H⁺-ATPase phosphorylation in GCPs. The upper blot displays the detection of the phosphorylation level of the H⁺-ATPase by immunoblot using the anti-phospho-Thr947 antibody (p-Thr). The lower blot shows detection of the H⁺-ATPase using a specific antibody against the C terminus of the H⁺-ATPase. Each lane contained 1.5 to 3.5 µg of guard cell proteins.

(D) Steady-state currents recorded under voltage clamp for $I_{K,in}$ and $I_{K,out}$ in isolated guard cells. Solid curves are fittings of the wild type ($n = 8$) and *amy3 bam1* ($n = 8$) to a Boltzmann function. Data are mean ± SE. The insets show measurements that were typically obtained by clamping in cycles with a holding voltage of −100 mV and 6-s steps either to voltages from −120 to −240 mV for $I_{K,in}$ or voltages from −80 to +40 mV for $I_{K,out}$.

(E) Instantaneous current voltage curves for I_{Cl} recorded in the wild type ($n = 8$) and *amy3 bam1* ($n = 11$). Data are means ± SE. Solid curve shows an empirical fitting to the second-order polynomial function and is included for clarity. The insets show representative I_{Cl} traces during 7-s clamp steps to voltages from +30 mV to −160 mV after a 10-s clamp step at +30 mV.
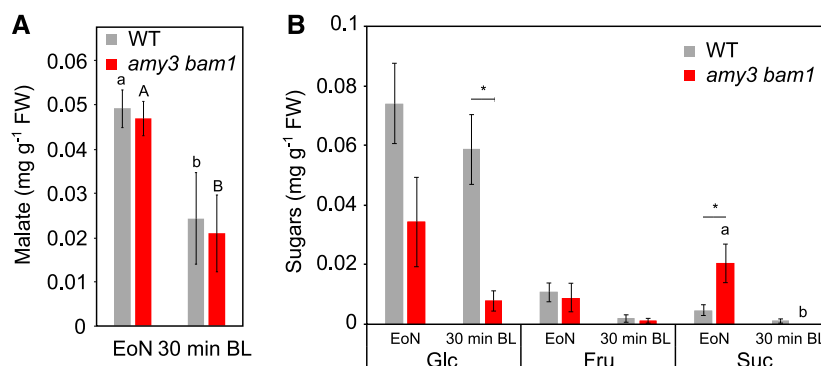
Figure 2. Metabolite Quantification in Wild-Type and *amy3 bam1* Guard Cells under BL.

Malate **(A)** and soluble sugar **(B)** contents of wild-type and *amy3 bam1* guard-cell–enriched epidermal peels at the EoN and after 30 min of incubation in stomatal opening buffer under 75 μmol m^{-2} s^{-1} of BL. FW, fresh weight. Data for two independent experiments are shown (means $\pm$ SE; $n \geq 6$). Different letters indicate statistically significant differences among time points for the given genotype. Asterisk (*) indicates statistically significant difference between genotypes for the given time point for P < 0.05 determined by one-way ANOVA with post hoc Tukey's test.

transport, and suggest that the rapid conversion of starch to Glc might directly influence g_s kinetics. To test this hypothesis, we examined kinetics of g_s and A in relation to guard cell starch dynamics in wild-type, *amy3 bam1*, and *aha1* plants. Given that loss of AHA1 H$^+$-ATPase in Arabidopsis impairs both membrane transport activities and starch metabolism (Horrer et al., 2016; Yamauchi et al., 2016), investigating the responses of *aha1* should help in understanding the interaction between metabolism and ion transport in the control of g_s kinetics. Plants were subjected to a two-pulsed–light treatment, during which plants were given pulses of light and darkness of 2 h each. This began at the EoN, after 30 min of dark adaptation under 150 μmol m^{-2} s^{-1} white light illumination, which is common for Arabidopsis (George et al., 2018). Given the purpose of our gas exchange measurements to compare stomatal opening kinetics between genotypes, g_s and A were normalized to the values at the EoN to facilitate the comparison of the velocity in the increase of the two parameters. Raw data for each experiment are provided in the Supplemental Figures.

Wild-type plants opened and closed their stomata in response to the alternating pulses of light and darkness (Figure 3A; Supplemental Figures 3A and 3B). However, stomatal opening during the second light pulse (4.5 h after dawn) was reduced and much slower compared with the first pulse (Figure 3B; Supplemental Figures 3A and 3B). Modeling the temporal responses of g_s to light consistently revealed a two-fold increase in the time constant, τ_i, for g_s response between the second and the first light pulse, corresponding to an increase in the half-time for opening of 19 min (Figure 3C); whereas the maximum slope (Sl_{max}), a parameter that combines rapidity and amplitude of the g_s response (Vialet-Chabrand et al., 2013), decreased by half (Figure 3D). The *amy3 bam1* and *aha1* mutants also responded to the fluctuations of light and darkness by opening and closing their stomata (Figure 3A; Supplemental Figures 3A and 3B), but their g_s kinetics were slow during both light pulses, particularly in the case of *amy3 bam1* (Figure 3A; Supplemental Figures 3C to 3H). Compared with the wild type, the *amy3 bam1* and *aha1* mutants showed significantly higher τ_i values for the first light pulse ($\tau_{i\,amy3\,bam1}$ = 57 $\pm$ 7 min; τ_{iaha1} = 25 $\pm$ 2 min; versus τ_{iWT} = 17 $\pm$ 1 min), with a concomitant reduction in Sl_{max}, corresponding to 10 min to 40 min slower opening

kinetics (Figures 3E and 3F; Supplemental Table 3). Note that the g_s responses to the second light pulse were similar between all genotypes, with calculated τ_i for opening of 36 $\pm$ 2 min for the wild type, 48 $\pm$ 4 min for *amy3 bam1*, and 56 $\pm$ 7 min for *aha1* (Figures 3A and 3C; Supplemental Figures 3E and 3F; Supplemental Table 3).

The differences in stomatal opening kinetics impacted on photosynthetic rates. A in the wild-type plants increased rapidly during the first light pulse and reached a final steady state after ~20 min of light, while A reached steady state only after ~50 min of light in response to the second light pulse (Figure 3G; Supplemental Figure 3I). Compared with the wild type, *amy3 bam1* mutants had lower A rates during the first light pulse (Figure 3G; Supplemental Figure 3I), in line with previous reports (Horrer et al., 2016). Estimations of C_i/C_a, describing the changes in the ratio of intercellular to ambient CO$_2$ concentrations throughout the treatment, assuming the resistance for CO$_2$ uptake being the same as for water efflux, confirmed that differences in photosynthetic rate in response to dark-to-light transition were driven largely by stomatal behavior. In wild-type plants, C_i/C_a values during the first pulse initially decreased when light was turned on due to photosynthetic consumption of CO$_2$, followed by an increase in C_i/C_a due to stomatal opening (Supplemental Figure 3J). In response to the second light pulse, C_i/C_a values after the initial drop increased more slowly due to the slower g_s kinetics (Supplemental Figure 3J). It is well established that light-induced activation of ribulose-1,5-bis-phosphate carboxylase/oxygenase influences the kinetics of A (Woodrow and Mott, 1989, 1992), particularly during the first 10 min, which is illustrated by the initial decrease in C_i/C_a. However, the absence of a difference in the C_i/C_a response during the first minutes of light between the two pulses and that the subsequent increase in C_i/C_a associated with the increase in g_s suggests stomatal limitation of A in our experimental conditions. The C_i/C_a dynamics in *amy3 bam1* and *aha1* plants followed a similar trend to that of the wild type, but *amy3 bam1* showed lower C_i/C_a values during the first light pulse due to the diffusive stomatal limitations imposed by the slow g_s responses (Supplemental Figure 3J).

As anticipated, rapid starch degradation occurred in wild-type guard cells during the first light pulse (Figure 3H). The second

stomatal opening was, surprisingly, associated with a net increase in starch content up until the middle of the light pulse, followed by starch mobilization (Figure 3H). In the case of the *amy3 bam1* mutant, starch content remained high for the entire duration of the experiment, with little or no turnover (Figure 3H). The *aha1* mutant showed an intermediate phenotype, with slight starch degradation occurring during the second half of both light pulses (Figure 3H). A possible explanation for this observation is that other H^+-ATPase isoforms may partially subsume the role of AHA1 in its absence. Consistent with this interpretation, we found that *AHA5* and to some extent *AHA2*, which are preferentially expressed in guard cells (Yamauchi et al., 2016), were upregulated in guard-cell–enriched epidermal peels of the *aha1* mutant when

compared with the wild type at the EoN (Supplemental Figure 4). Altogether, these results show that the differences in stomatal opening kinetics between the first and the second light pulse in the wild type, and between the wild type and the mutants, which affected *A* rates, were consistent with the underlying differences in guard cell starch metabolism. As a control, we measured starch content in the leaves, and found no differences between the wild type and the mutants (Supplemental Figure 5). In all cases, starch accumulation occurred in the light, while only a modest degradation of starch was observed in the wild type in response to the second dark period 6.5 h after dawn (Supplemental Figure 5). Thus, the delayed starch degradation in the wild-type guard cells during the second light pulse (Figure 3H) can explain the slow opening response.
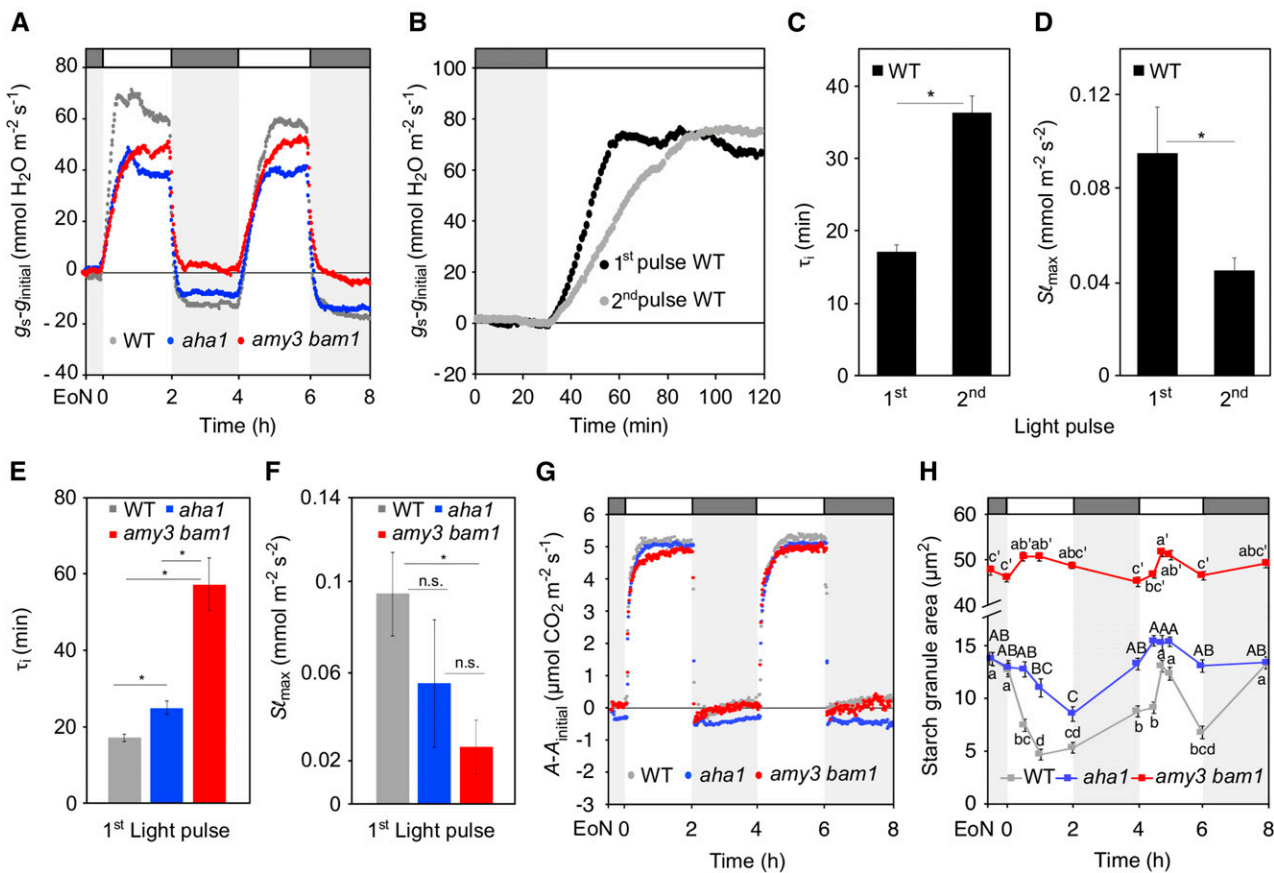

Figure 3. Stomatal Opening Kinetics and Guard Cell Starch Dynamics in Plants Subjected To a Two-Pulsed–Light Treatment.

(A) Normalized whole-plant recordings of g_s–$g_{initial}$ values in dark-adapted (30 min) plants in response to 2-h L, 2-h D, 2-h L, and 2-h D (L, light; D, darkness). Plants were illuminated with 150 μmol m^{-2} s^{-1} white light. The g_s values were normalized to values at the EoN. Number of measured plants per genotype $n \geq$ 3; values presented are means. WT, wild type.

(B) Changes in g_s–$g_{initial}$ values in response to a shift from dark to light in wild-type plants. Data are taken from **(A)**.

(C) to **(F)** Rapidity of the stomatal response estimated using a time constant (τ **[C]**) and the maximum slope of g_s increase (Sl_{max}, **D**) during the two consecutive pulses of light in the wild type (**[C]** and **[D]**) and during the first pulse in all three genotypes (**[E]** and **[F]**). Unpaired student's *t* test determined statistical significance between the indicated comparisons (*P < 0.05; n.s., not significant).

(G) Normalized whole-plant recordings of A-$A_{initial}$ values from plants under the same light regime as given in **(A)**. Values for A were normalized to values at the EoN. Number of measured plants per genotype $n \geq$ 3; values presented are means.

(H) Guard cell starch dynamics of plants under the same light regime as given in **(A)**. Each value represents mean $\pm$ SE of three biological replicates of >110 individual guard cells obtained from three independent experiments. Different letters indicate statistically significant differences among time points for the given genotype for P < 0.05 determined by one-way ANOVA with post hoc Tukey's test.
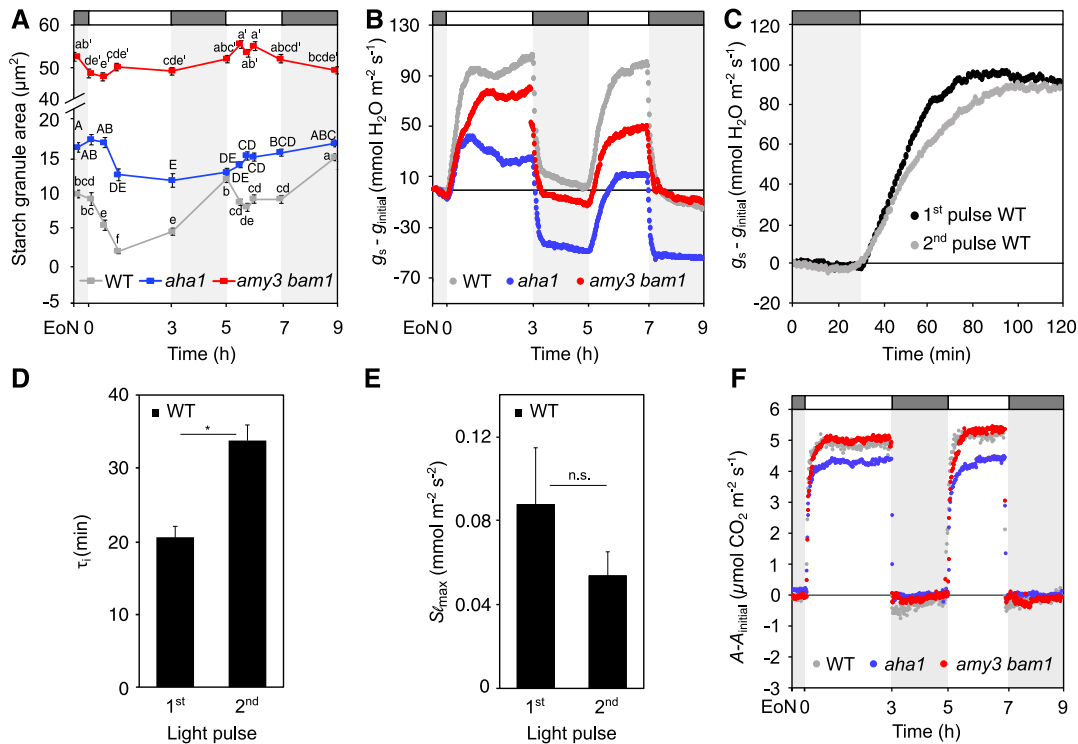
Figure 4. Stomatal Opening Kinetics and Guard Cell Starch Dynamics in Plants Subjected to a Modified Two-Pulsed–Light Treatment.

(A) Guard cell starch dynamics in dark-adapted (30 min) plants in response to 3-h L, 2-h D, 2-h L, and 2-h D (L, light; D, darkness). Plants were illuminated with 150 μmol m^{-2} s^{-1} white light. Each value represents mean $\pm$ SE of three biological replicates of >110 individual guard cells obtained from three independent experiments. Different letters indicate statistically significant differences among time points for the given genotype for P < 0.05 determined by one-way ANOVA with post hoc Tukey's test. WT, wild type.

(B) Normalized whole-plant recordings of g_s–$g_{initial}$ values in plants exposed to the same light regime as given in **(A)**. The g_s values were normalized to values at the EoN. Number of measured plants per genotype $n \geq 3$; values presented are means.

(C) Changes in g_s–$g_{initial}$ values in response to a shift from dark to light in wild-type plants. Data are replotted from **(B)**.

(D) and **(E)** Rapidity of the stomatal response estimated using a time constant (τ **[D]**) and the maximum slope of g_s increase (Sl_{max} **[E]**) during the two consecutive pulses of light in the wild type. Unpaired Student's t test determined statistical significance between the indicated comparisons (*P < 0.05; n.s., not significant).

(F) Normalized whole-plant recordings of A-$A_{initial}$ values from plants under the same light regime as given in **(B)**. Values for A were normalized to values at the EoN. Number of measured plants per genotype $n \geq 3$; values presented are means.

To test the connection between guard cell starch degradation and g_s kinetics further, we extended the length of the first light pulse from 2 to 3 h (Figure 4). We reasoned that guard cell starch content might recover sufficiently to reach a threshold level that would allow immediate starch breakdown at the onset of the second light pulse and again promote fast stomatal opening. Indeed, in response to this modified two-pulsed–light treatment, wild-type guard cells degraded starch at the beginning of the second pulse (occurring this time 5.5 h after dawn; Figure 4A), and stomata opened more rapidly (Figures 4B and 4C; Supplemental Figures 6A and 6B). The changes in τ_i and Sl_{max} between the second and the first light pulse this time corresponded to a reduction in the half-time for opening of 13 min (Figures 4D and 4E; Supplemental Table 3), showing that by extending the first light pulse, opening during the second was accelerated by almost 7 min when compared with the original two-pulsed–light treatment (Figures 4C and 4D; Supplemental Table 3). In line with the g_s kinetics, we observed no differences in A and C_i/C_a dynamics

between the second and the first pulse (Figure 4F; Supplemental Figures 6I and 6J).

By contrast, the pattern of starch accumulation in the *amy3 bam1* and *aha1* mutants remained unchanged, resembling that of the original two-pulsed–light treatment (Figure 4A versus Figure 3H) and again resulted in reduced stomatal opening with slow g_s kinetics compared with the wild type (Figure 4B; Supplemental Figures 6A to 6G). The *aha1* mutant also showed a decrease in g_s amplitude roughly 2.5 h after dawn, suggesting that this mutant does not maintain the stomata open under prolonged illumination (Figure 4B). As a result, A rates in *aha1* were reduced, particularly during the second light pulse (Figure 4F). The C_i/C_a dynamics followed a similar trend to that of wild-type plants, but this time both *aha1* and *amy3 bam1* mutants showed reduced C_i/C_a values compared to the wild type after the initial drop (Supplemental Figure 6J), matching the extremely slow g_s kinetics and reduced amplitude (Figure 4B; Supplemental Figures 6A to 6H). This further highlights how changes in C_i/C_a dynamics are linked to g_s kinetics.

Taken together, our two-pulsed–light experiments and guard cell metabolite measurements suggest that the acceleration of stomatal opening above a baseline rate is associated with the amount of starch that is degraded to Glc, presumably needed to maintain proper guard cell sugar homeostasis.

Guard Cell Starch Dynamics in Response to Changes in Light Regime Do Not Depend on the Time of Day

To examine whether the changes in starch dynamics in response to the extension of the first light pulse from 2 to 3 h might simply reflect a time-of-day–dependent effect on guard cell starch metabolism, we subjected wild-type plants to a second regime of modified two-pulsed–light treatment. The first light pulse (2 h) was followed by 3 h of darkness, such that the beginning of the second light pulse still occurred 5.5 h after dawn (Figure 5). Under these conditions, stomatal opening during the second light pulse was accompanied by substantial guard cell starch accumulation, resulting in slow g_s kinetics (Figures 5A to 5C; Supplemental Figure 7A). The time constant of the second pulse increased 4-fold, while the maximum slope decreased by 2.6-fold, corresponding to an increase in the half-time for stomatal opening of ~1 h (Figures 5D and 5E). A was also affected by the change in the light treatment, showing slower rates compared with the first light
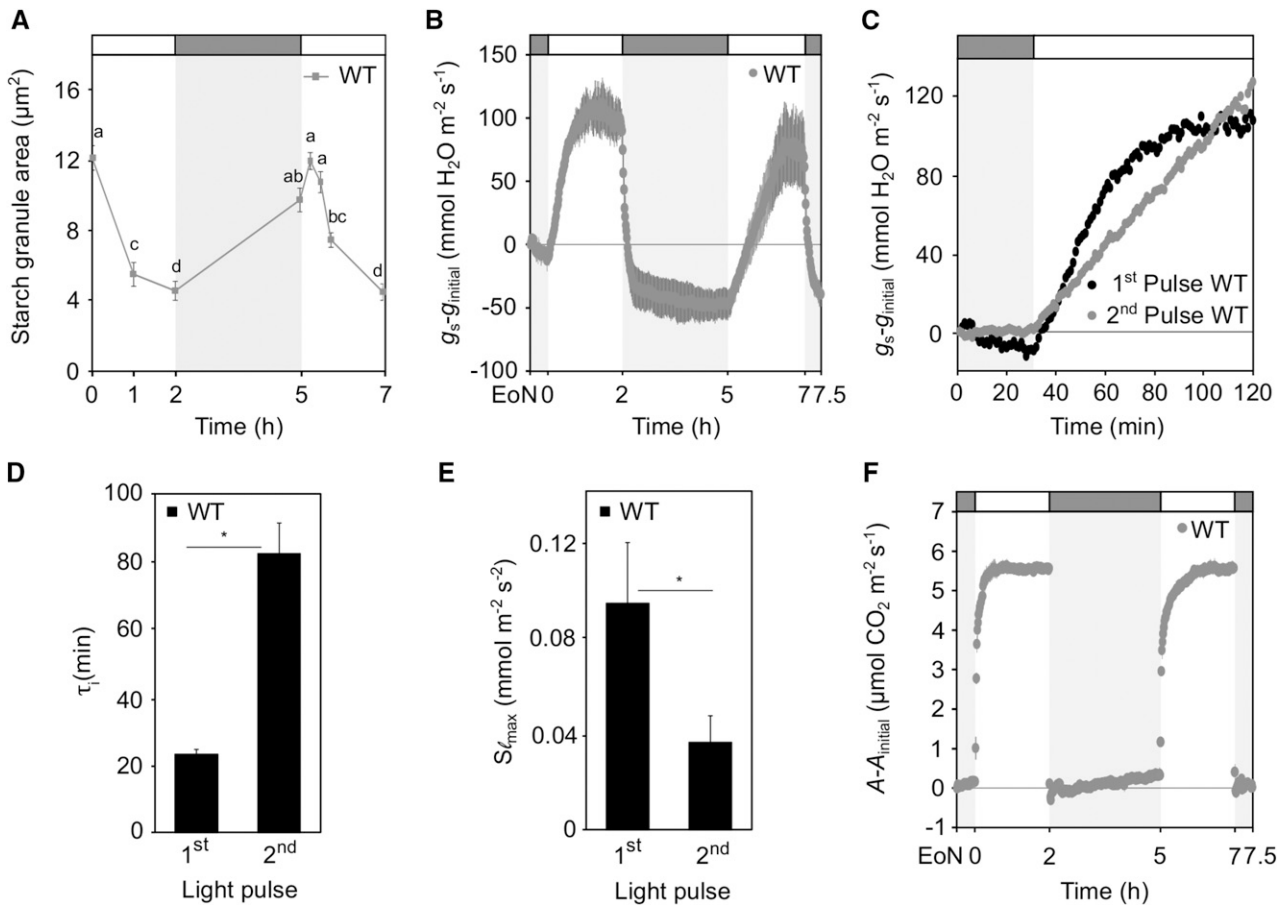

Figure 5. Effect of Time of Day on Guard Cell Starch Metabolism and Stomatal Kinetics.

(A) Guard cell starch dynamics in dark-adapted (30 min) plants in response to 2-h L, 3-h D, 2-h L, and 2-h D (L, light; D, darkness). Plants were illuminated with 150 μmol m^{-2} s^{-1} white light. Each value represents mean $\pm$ SE of three biological replicates of >110 individual guard cells obtained from three independent experiments. Different letters indicate statistically significant differences among time points for the given genotype for P < 0.05 determined by one-way ANOVA with post hoc Tukey's test. WT, wild type.

(B) Normalized whole-plant recordings of changes in g_s–$g_{initial}$ in plants exposed to the same light regime as given in **(A)**. The g_s values were normalized to values at the EoN, $n = 3$; values presented are means $\pm$ SE.

(C) Changes in g_s–$g_{initial}$ in response to a shift from dark to light in wild-type plants. Data are replotted from **(B)**.

(D) and **(E)** Rapidity of the stomatal response estimated using a time constant (τ **[D]**) and the maximum slope of g_s increase (Sl_{max} **[E]**) during the two consecutive pulses of light in the wild type. Unpaired Student's t test determined statistical significance between the indicated comparisons (*P < 0.05; n.s., not significant).

(F) Normalized whole-plant recordings of A-$A_{initial}$ values from plants under the same light regime as given in **(A)**. Values for A were normalized to values at the EoN, $n = 3$; values presented are means $\pm$ SE.
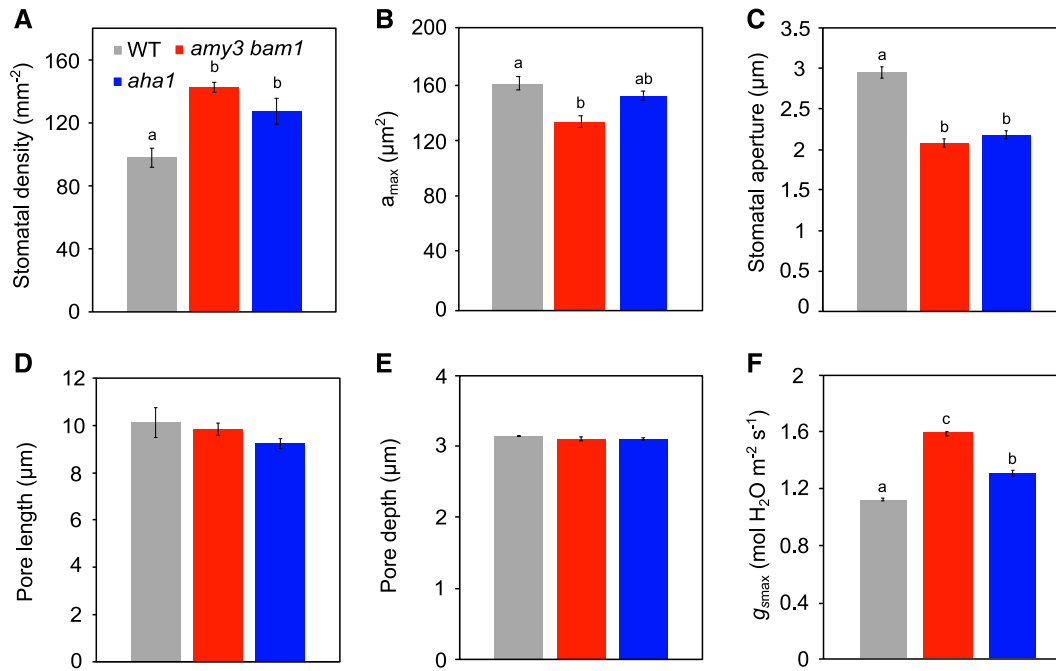
Figure 6. Stomatal Anatomical Features.

Stomatal physical attributes of wild-type, *amy3 bam1*, and *aha1* plants were determined using micrographs of epidermal peels from the abaxial side of leaf number 6, harvested 2 h into the light phase.

(A) Stomatal density.

(B) Stomatal pore size (a_{max}).

(C) Stomatal aperture.

(D) Pore length.

(E) Pore depth.

(F) Anatomical maximum g_{smax} as determined by stomatal size and density. Data are means ± SE of $n = 365$ stomata for the wild type, $n = 377$ stomata for *aha1*, and $n = 481$ stomata for *amy3 bam1* from three independent experiments. Different letters indicate statistically significant differences among genotypes for $P < 0.05$ determined by one-way ANOVA with post hoc Tukey's test.

pulse (Figure 5F; Supplemental Figure 7B). Thus, the rearrangements of guard cell starch metabolism observed in our experiments were directly linked to the applied light regime, excluding the possibility that the decline in starch content in response to the second light pulse in the modified two-pulsed–light treatment (Figure 4A) was affected by the time of day.

Stomatal Anatomical Features of *amy3 bam1* and *aha1* Mutants Do Not Explain Their Slow g_s Kinetics

We also examined foliar stomatal anatomy to assess its contribution to the altered g_s response to light of *amy3 bam1* and *aha1* mutants. For this purpose, we calculated the maximum theoretical conductance (g_{smax}). Anatomical g_{smax} defines the potential maximum rate of g_s to water vapor as determined by the size and density of stomata in a diffusion-based equation (Dow et al., 2014). Compared with the wild type, both *amy3 bam1* and *aha1* mutant plants had more stomata per unit leaf area (143 ± 3 mm^{-2} and 127 ± 8 mm^{-2}, respectively, versus 98 ± 6 mm^{-2}; Figure 6A). They also showed a smaller pore area (a_{max}; 152 ± 4 μm^2 for *amy3 bam1* and 134 ± 3 μm^2 for *aha1* compared with 161 ± 5 μm^2 for the wild type; Figure 6B), primarily because of a smaller aperture rather

than reductions in pore length or depth (Figures 6C to 6E), indicating that the guard cell membrane surface in *amy3 bam1* and *aha1* was likely similar to that of the wild type. The physical attributes of *amy3 bam1* and *aha1* with highly dense stomata and smaller pore area should theoretically allow increased stomatal conductance values compared with the wild type (Drake et al., 2013). Indeed, our calculations yielded significantly higher g_{smax} values for both mutants (Figure 6F). The higher g_{smax} of the *amy3 bam1* and *aha1* mutants, however, did not match the observed g_s responses. These results suggest that the effect of starch and proton pumping on g_s kinetics of Arabidopsis stomata is independent of anatomical features such as size and density. We interpret the elevated density of stomata in *amy3 bam1* and *aha1* mutants as an adaptive developmental response to the limited capacity to open the pore.

Fast g_s Kinetics under Saturating Photosynthetic Active Radiation Are Independent of Guard Cell Starch Degradation, But Require the PM H$^+$-ATPase

It is well established that guard cell osmoregulation is driven by different processes depending on the light quality and intensity
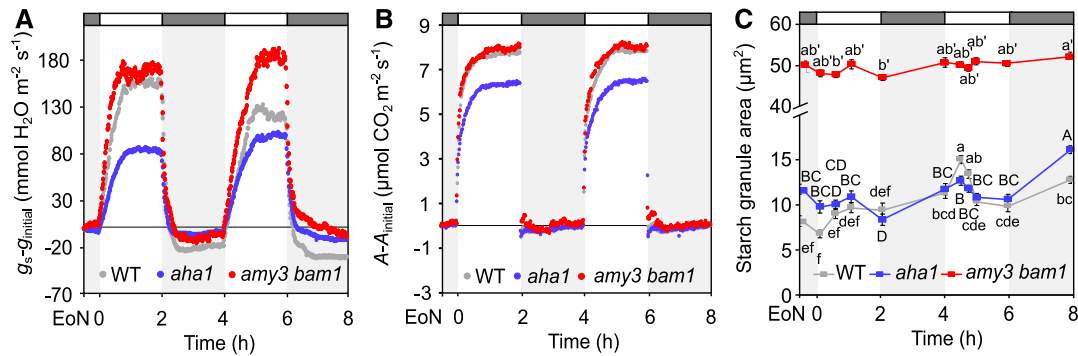
Figure 7. Effect of Saturating Photosynthetic Active Radiation on Guard Cell Starch Metabolism and Stomatal Kinetics.

(A) Normalized whole-plant recordings of g_s–$g_{initial}$ in dark-adapted (30 min) plants in response to 2-h L, 2-h D, 2-h L, and 2-h D (L, light; D, darkness). Plants were illuminated with 400 μmol m^{-2} s^{-1} white light. The g_s values were normalized to values at the EoN. Number of measured plants per genotype $n \geq 3$; values presented are means. WT, wild type.

(B) Normalized whole-plant recordings of A-$A_{initial}$ values from plants under the same light regime as given in **(A)**. Values for A were normalized to values at the EoN. Number of measured plants per genotype $n \geq 3$; values presented are means.

(C) Guard cell starch dynamics of plants under the same light regime as given in **(A)**. Each value represents mean $\pm$ SE of three biological replicates of >110 individual guard cells obtained from three independent experiments. Different letters indicate statistically significant differences among time points for the given genotype for P < 0.05 determined by one-way ANOVA with post hoc Tukey's test.

(Talbott and Zeiger, 1996). The early morning BL response, which is nonphotosynthetic, is associated with H$^+$-ATPase-dependent uptake of K$^+$ and Cl$^-$, synthesis/uptake of Mal, and degradation of starch (Outlaw and Lowry, 1977). The photosynthetic or RL response, which is induced by light intensities that saturate photosynthesis, is supposed to be accompanied by an increased sugar concentration, mainly Suc (Talbott and Zeiger, 1993), and to be independent of starch degradation (Poffenroth et al., 1992). Furthermore, g_s is determined by the capacity of the mesophyll tissue to fix carbon (Wong et al., 1979).

To test further the connection between guard cell starch degradation and stomatal opening kinetics under light intensities that saturate photosynthesis (400 μmol m^{-2} s^{-1} for Arabidopsis; George et al., 2018), we subjected wild-type, *amy3 bam1*, and *aha1* plants to a typical two-pulsed–light treatment with alternating pulses of white light and darkness of 2 h each with a light intensity of 400 μmol m^{-2} s^{-1}.

Under these conditions, all genotypes achieved higher steady-state g_s compared with plants illuminated with 150 μmol m^{-2} s^{-1} (Figure 7A; Figures 3A and 4B for comparison), and a greater A (Figure 7B; Figures 3G and 4F for comparison). Wild-type stomata opened rapidly in response to both light pulses, with the speed of g_s responses resembling those of the first pulse at a fluence rate of 150 μmol m^{-2} s^{-1} (Figure 7A; Supplemental Figures 8A to 8C). However, in this case, stomatal opening in the wild type was accompanied by starch accumulation (Figure 7C), suggesting that when plants are carbon-saturated, fast stomatal opening kinetics are independent of guard cell starch degradation and its derived metabolites.

This observation was supported by data from the *amy3 bam1* mutant. Guard cell starch dynamics in this mutant were unaffected by the changes in light intensity, and starch content remained high throughout the experiment (Figure 7C). Nonetheless, g_s responses were similar to the wild type: the *amy3 bam1* mutant showed rapid increases in g_s as well as wild-type–like A rates and C_i/C_a values

(Figures 7A and 7B; Supplemental Figures 8A to 8D). Surprisingly, under these saturating light intensities, the g_s response of the *aha1* mutant differed from that of the *amy3 bam1* mutant. The *aha1* mutant displayed slower stomatal opening kinetics and reduced steady-state g_s during both light periods, which resulted in lower A rates (Figures 7A and 7B; Supplemental Figure 8E and 8F). The *aha1* mutant also showed reduced C_i/C_a values compared with the wild type and the *amy3 bam1* mutant (Supplemental Figure 8G). The fact that *amy3 bam1*, but not *aha1*, behaved similar to the wild type suggests that: (1) carbon sources for stomatal opening under photosynthesis-saturating light conditions do not derive from starch degradation, and (2) photosynthesis-driven opening response depends on the activity of the PM H$^+$-ATPase.

PM H$^+$-ATPase Activity Is Required for Fast Stomatal Opening Kinetics and Guard Cell Starch Accumulation under RL

To uncover the reasons for the stomatal phenotype of *aha1* under saturating white light irradiation, we examined stomatal opening kinetics under RL, which avoids the nonphotosynthetic BL responses (Shimazaki et al., 2007). The RL response is abolished by 3-(3,4-dichlorophenyl)-1,1-dimethylurea (an inhibitor of PSII; Olsen et al., 2002; Messinger et al., 2006), and, by contrast to BL, is associated with net guard cell starch accumulation (Tallman and Zeiger, 1988; Horrer et al., 2016).

As anticipated, illumination of wild-type plants with 300 μmol m^{-2} s^{-1} of RL resulted in rapid stomatal opening with elevated steady-state g_s, and was accompanied by efficient guard cell starch accumulation, which was sustained for the entire duration of the treatment (Figures 8A and 8B; Supplemental Figures 9A to 9C). Compared to the wild type, both *amy3 bam1* and *aha1* mutants showed reduced g_s amplitude, with *aha1* having exceptionally slow g_s kinetics (Figure 8A; Supplemental Figures 9A to 9C). The *aha1* mutant also showed no changes in guard cell starch
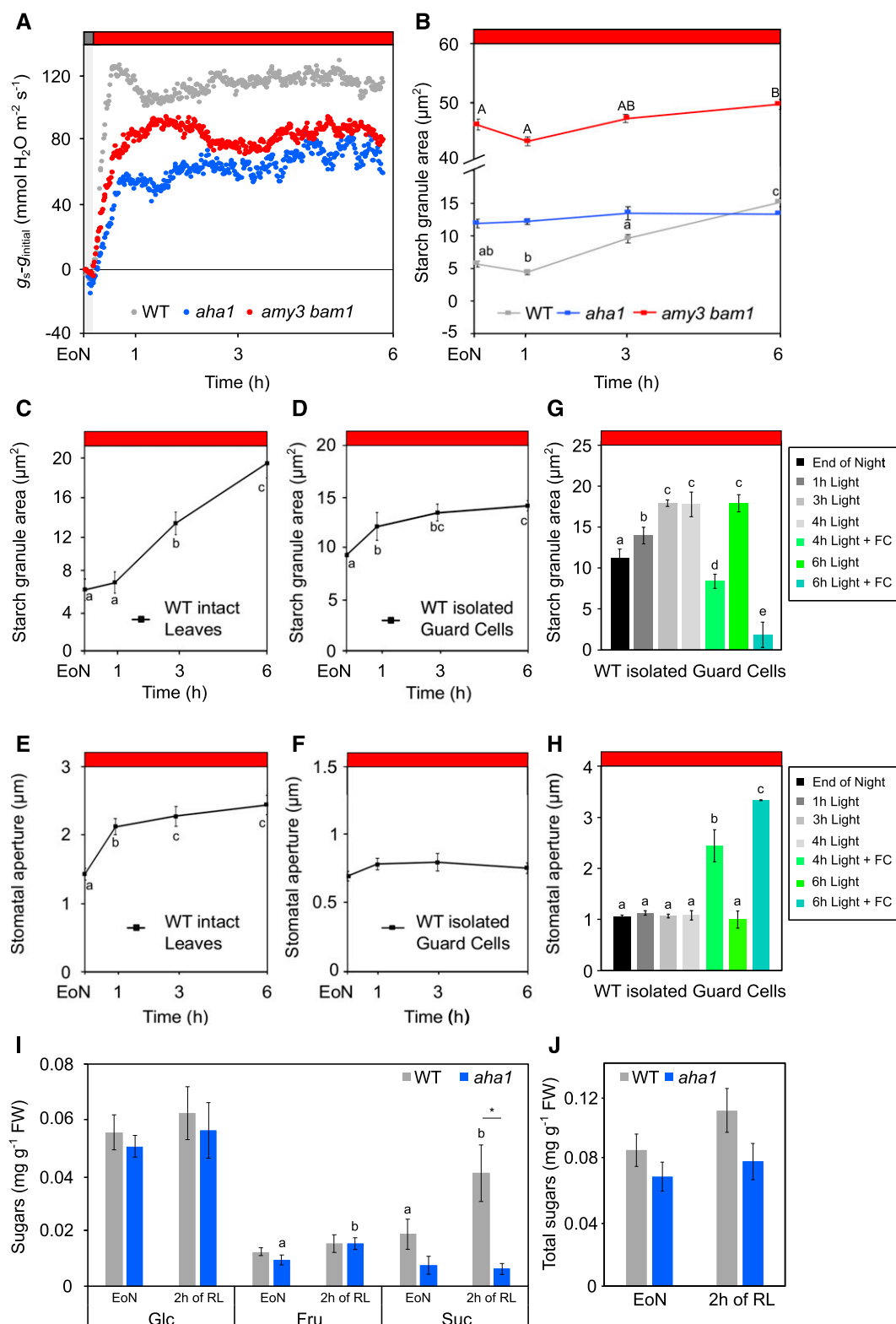
Figure 8. Effect of RL on Guard Cell Carbohydrate Metabolism and Stomatal Kinetics.

(A) Normalized whole-plant recordings of g_s–$g_{initial}$ in dark-adapted (30 min) plants in response to 6-h illumination with 300 μmol m^{-2} s^{-1} of RL. The g_s values were normalized to values at the EoN, $n = 3$; values presented are means. WT, wild type.

content, while the *amy3 bam1* had slight, but significant net increase in starch levels (Figure 8B). These differences, however, did not affect *A* rates, which were similar in all three genotypes (Supplemental Figures 9D and 9E).

Based on these observations and earlier research suggesting that stomatal opening under saturating light likely depends on the import of mesophyll-derived sugars (Poffenroth et al., 1992), we reasoned that the differences in starch accumulation under RL between the wild type and *aha1* may reflect the capacity of their guard cells to import apoplastic sugars.

Firstly, we compared the ability to accumulate starch in response to RL of wild-type guard cells of intact leaves and wild-type guard cells in isolated epidermal peels in which there is no connection with the mesophyll. We observed starch accumulation in both cases; however, guard cells of intact leaves, despite a short delay in the onset of synthesis, accumulated substantially more starch than isolated guard cells, showing a 4-fold increase in starch content by the end of the treatment (Figures 8C and 8D). We also observed that stomata of intact leaves efficiently opened in response to RL, whereas isolated stomata remained closed (Figures 8E and 8F). To verify that the isolated guard cells were still responsive to external stimuli after floating for several hours in the buffer, we performed a control experiment in which we treated isolated peels with fusicoccin (Fc). Fc is a chemical activator of the PM H^+-ATPase and, in turn, of guard cell starch degradation (Horrer et al., 2016). After 3 h of RL illumination, exogenous application of Fc resulted in efficient starch degradation and induction of stomatal opening, as determined after 1 h and 3 h of treatment (Figures 8G and 8H). Altogether, these findings show that starch in guard cells under RL is made primarily from imported sugars; and they further support the idea that a mesophyll-derived signal (presumably sugars) is required for RL-induced stomatal opening (Lee and Bowling, 1992; Mott et al., 2008).

Having established the importance of mesophyll-derived sugars for RL-mediated responses, we next determined soluble sugar content in wild-type and *aha1* guard cells of intact leaves at the EoN and after 2 h of RL illumination (300 μmol m^{-2} s^{-1}). Glc and Fru levels were similar in the two genotypes and remained constant under RL (Figure 8I; Supplemental Table 4). Notably, Suc

levels at the EoN were 2-fold higher in the wild type compared to *aha1* (Figure 8I; Supplemental Table 4) and Suc doubled in wild-type guard cells under RL, whereas it remained low in *aha1* (Figure 8I; Supplemental Table 4). Quantification of total amount of soluble sugars further showed that in wild-type guard cells, sugar content rose under RL by ~30%, but only ~12% in *aha1* (Figure 8J).

Taken together, the severely impaired g_s kinetics of *aha1* under RL, along with impaired guard cell Suc accumulation and lack of starch synthesis, strongly suggest that the RL stomatal response depends on Suc supply from the mesophyll and that the uptake of mesophyll-derived Suc is mediated by the PM H^+-ATPase, presumably via energization of Suc transporters.

DISCUSSION

Integration of Guard Cell Starch Metabolism with Membrane Ion Transport during BL-Induced Stomatal Opening

Loss of AHA1 H^+-ATPase in Arabidopsis directly translates into a reduction of proton extrusion by the guard cells, impairing both membrane transport activities and starch metabolism, and causing reduced stomatal opening (Horrer et al., 2016; Yamauchi et al., 2016). Despite this seemingly tight connection between guard cell starch metabolism and ion transport, here we showed that starch degradation does not directly affect H^+ flux or the capacity for K^+ and Cl^- transport (Figure 1; Supplemental Figure 1). These findings have important implications. Firstly, besides the energy stored in starch, other metabolic processes, such as the electron transport chain in the chloroplast (Suetsugu et al., 2014), oxidative phosphorylation in mitochondria (Daloso et al., 2015), or BL-dependent β-oxidation of lipids (McLachlan et al., 2016), can contribute to the energy requirements of stomatal opening. Secondly, the presence of a functional H^+-ATPase and of unaffected K^+ and Cl^- channel currents in *amy3 bam1* show that their transport activities alone do not limit light-induced stomatal opening. We found the *amy3 bam1* mutant capable of driving H^+ flux like the wild type under BL illumination and

---

Figure 8. (continued).

(B) Starch accumulation in guard cells.

(C) Starch content in wild-type guard cells of intact leaves.

(D) Starch content in wild-type isolated guard cells.

(E) Stomatal aperture in wild-type guard cells of intact leaves.

(F) Stomatal aperture in wild-type isolated guard cells.

(G) Starch content in wild-type isolated guard cells with or without treatment (10 μM of Fc applied after 3 h of light exposure).

(H) Stomatal aperture in wild-type isolated guard cells with or without treatment (10 μM of Fc; applied after 3 h of light exposure).

(I) Soluble sugar and **(J)** total sugar contents of wild-type and *aha1* guard-cell–enriched epidermal peels at the EoN and after 2-h illumination with 300 μmol m^{-2} s^{-1} of RL. Data for two independent experiments are shown (means $\pm$ SE; $n \geq 11$). FW, fresh weight.

(B) to **(D)** and **(G)** Same light conditions as given in **(A)**. Each value represents mean $\pm$ SE of three biological replicates of >110 individual guard cells obtained from three independent experiments. Different letters indicate statistically significant differences among time points for the given genotype. Asterisk (*) indicates statistically significant difference between genotypes for the given time point for P < 0.05 determined by one-way ANOVA with post hoc Tukey's test.

(E) to **(H)** Same light conditions as given in **(A)**. Each value represents mean $\pm$ SE of four biological replicates of >200 individual stomata obtained from two independent experiments. Different letters indicate statistically significant differences among time points for the given genotype. Asterisk (*) indicates statistically significant difference between genotypes for the given time point for P < 0.05 determined by one-way ANOVA with post hoc Tukey's test.

sufficient to energize the ion uptake needed for the increase in inorganic solute content during stomatal opening (Wang et al., 2012, 2017; Jezek and Blatt, 2017), yet g_s increased only slowly in response to BL (10 μmol m^{-2} s^{-1}) superimposed on RL (50 μmol m^{-2} s^{-1}; Supplemental Figure 1B). We conclude that starch degradation in guard cells is not primarily required for energy production to drive stomatal opening, and does not directly affect the ability of membrane ion transport.

Glc Is the Major Starch-Derived Metabolite during BL-Induced Stomatal Opening

In the early 20th century, starch-to-sugar conversion was the most widely accepted theory explaining the osmotic changes leading to alterations in guard cell turgor (Lloyd, 1908; Scarth, 1927). However, soon after the importance of K$^+$ in stomatal movement was revealed (Fischer, 1968; Fischer and Hsiao, 1968), the starch–sugar theory was put aside. Since then, K$^+$ has been recognized as the major osmoticum in guard cells, with Mal and/or Cl$^-$ and nitrate acting as the counterions (Humble and Raschke, 1971; Allaway, 1973; Outlaw and Lowry, 1977; Travis and Mansfield, 1977; Schnabl and Raschke, 1980). According to this model, Mal is synthesized within the guard cells using starch as a source of carbon skeletons. Experimental support for this model comes from studies in *Vicia faba* linking changes in GCP volume to changes in Mal and starch contents. Mal was determined enzymatically in GCPs incubated under white light and CO_2-free air (Schnabl, 1980a, 1980b; Schnabl et al., 1982). Further studies have reported an increase in Mal content in guard cells due to white light illumination (Allaway, 1973; Travis and Mansfield, 1977). These reports are based on measurements from *V. faba* or *Commelina communis* guard cells of intact leaves (Allaway, 1973) or epidermal fragments (Travis and Mansfield, 1977), not excluding the possibility of Mal import from the mesophyll.

Here, we quantified enzymatically Mal and sugars in wild-type and *amy3 bam1* isolated guard cells before and after floating them in opening buffer under BL for 30 min. We showed that defective starch degradation in *amy3 bam1* had no impact on Mal accumulation in guard cells at the EoN and after the BL treatment when compared to the wild type (Figure 2A; Supplemental Table 1). In response to BL illumination, Mal decreased in both genotypes (Figure 2A; Supplemental Figure 2A), indicating that Mal is a substrate for BL-induced stomatal opening in Arabidopsis. However, we cannot exclude that a transient peak in Mal accumulation was missed due to our experimental setup. Simultaneous synthesis and use of Mal in guard cells makes it difficult to detect fine changes in the amount of this metabolite. The fact that there were no differences in Mal content between the wild type and *amy3 bam1* leads us to conclude that Mal is not the major starch-derived metabolite in Arabidopsis guard cells during BL-induced stomatal opening.

Sugar homeostasis, on the other hand, was dramatically altered in *amy3 bam1* guard cells. Already at the EoN, *amy3 bam1* had half as much Glc as the wild type, but accumulated 4-fold more Suc (Figure 2B). After the BL treatment, Glc (7-fold less than the wild type) was almost undetectable, while wild-type guard cells still contained high amounts of Glc (Figure 2B; Supplemental Table 2). This was not the case if isolated guard cells were dark-incubated for 30 min (Supplemental Figure 2C). Glc levels in both genotypes decreased during darkness, demonstrating that Glc derives from guard cell starch degradation specifically under BL.

These unexpected findings suggest that Glc is the major-starch derived metabolite in Arabidopsis guard cells. We conclude that it is unlikely that Mal is synthesized from carbon skeletons derived from starch degradation, and propose that Mal is more likely produced from anaplerotic CO_2 fixation within the guard cells (Asai et al., 2000; Robaina-Estévez et al., 2017) or directly imported from the apoplast via the ABC transporter ABCB14 (Lee et al., 2008) to fulfill its function as an allosteric activator, counterion, and osmotically active solute.

Even though the starch-sugar hypothesis got short shrift, recent evidence has again pointed to the significance of carbohydrates, in addition to K$^+$ and anions, during the build-up of the guard cell turgor (reviewed by Daloso et al., 2016, 2017; Santelia and Lawson, 2016; Santelia and Lunn, 2017; Lima et al., 2018; Granot and Kelly, 2019). Our data further support this view. A first consideration is that ion transport across the PM requires a significant amount of energy in the form of ATP. One of the roles of guard cell carbohydrate metabolism is to meet this energetic demand. Suc was long thought to act as an osmolyte (Poffenroth et al., 1992; Talbott and Zeiger, 1993; Amodeo et al., 1996), but more recent reports suggest that Suc is broken down to fuel the tricarboxylic acid cycle and provide energy for stomatal opening (Daloso et al., 2015, 2016; Medeiros et al., 2018). In line with this hypothesis, we observed, in both wild-type and *amy3 bam1* guard cells, Suc depletion under light (Figure 2B) but not in darkness (Supplemental Figure 2C). A second consideration is that sequestration of K$^+$ in the vacuole (in the form of K$_2$Mal or KCl) requires cytosolic volume to be maintained. This can be achieved through import or synthesis of sugars. Thus, the cytoplasmic sugar pool must be replenished during stomatal opening to maintain cellular homeostasis and provide carbon skeletons for energy production. The reduced levels of Glc along with the slow and reduced stomatal opening in *amy3 bam1* suggests that fast starch degradation at dawn is required for sufficient and continuous provision of sugars. Reduced levels of Glc in *amy3 bam1* invokes compensatory Suc uptake and may explain why, at the EoN, *amy3 bam1* accumulated 4-fold more Suc than the wild type along with the increased amount of available Suc from *amy3 bam1* mesophyll cells.

The metabolic pathways within the mitochondria, chloroplasts, and cytosol are in a delicate balance. The rapid conversion and exchange of metabolites between these subcellular compartments is a cardinal event in guard cells, which ultimately coordinate the energetic and metabolic status of the cell with membrane ion transport activity.

BL-Induced Guard Cell Starch Degradation Promotes Fast Stomatal Opening Kinetics under Common Lighting Conditions

In response to fluctuations in environmental parameters, plants try to coordinate stomatal opening with the mesophyll demand for CO_2 and stomatal closure with the need to minimize water loss through transpiration. An important limitation in this process is the rate at which stomata open and close, which is usually more than an order-of-magnitude slower compared with photosynthetic

responses (Lawson and Blatt, 2014; Lawson and Vialet-Chabrand, 2019). The intercellular CO_2 concentration (C_i) was long considered to be the factor mediating the coordination between A and g_s (reviewed in Lawson et al., 2014). However, recent research reporting increases in g_s with light despite high C_i or after reaching steady-state A (Lawson et al., 2008; Matrosova et al., 2015) raises questions about the role of C_i as primary driver of A-g_s coordination. Furthermore, there is increasing evidence that for species with kidney-shaped stomata, such as Arabidopsis, anatomical features, including size and density, are not directly correlated with the speed nor the amplitude of stomatal responses (Franks and Farquhar, 2007; Elliott-Kingston et al., 2016; McAusland et al., 2016).

Therefore, it has been hypothesized that characteristics other than stomatal anatomy may influence the g_s kinetics in this type of stomata (McAusland et al., 2016).

In this study, we provide evidence that identifies guard cell starch metabolism as a key determinant of fast stomatal opening kinetics under common light conditions. We show that guard starch degradation in Arabidopsis helps to accelerate stomatal opening above a baseline rate. The temporal responses of g_s to light showed that inhibiting guard cell starch degradation in *amy3 bam1* or *aha1* mutants resulted in slow stomatal opening kinetics compared to the wild type, with a calculated increase in the time constant for opening of up to 40 min (Figures 3E and 3F). The fact that the *amy3 bam1* and *aha1* mutants have a higher potential g_{smax}, despite the observed reduced g_s amplitude (Figure 6F), further demonstrates that the effect of starch on g_s of Arabidopsis stomata was independent of size and density. Similar alterations in anatomical features that cannot explain the different temporal responses of g_s were found in other mutants, such as the outward rectifying K^+ channel mutant *gork1-1* (Vialet-Chabrand et al., 2017a). Thus, metabolism—and its coordination with membrane ion transport—overrides anatomy in the control of stomatal opening kinetics in kidney-shaped stomata. We propose that the manipulation of g_s kinetics by controlling guard cell starch dynamics could be a potential tool to improve the coordination of stomatal opening with mesophyll demand for CO_2 that may be exploited to enhance plant WUE.

H^+-ATPase Energizes Sugar Uptake for Fast g_s Kinetics during Photosynthesis-Mediated Stomatal Responses

We showed that when plants are photosynthetic-rate–saturated (i.e., at 400 μmol m^{-2} s^{-1} of light), fast stomatal opening kinetics are independent of guard cell starch degradation. Consistent with this idea, the *amy3 bam1* mutant showed g_s responses similar to the wild type when illuminated with 400 μmol m^{-2} s^{-1} of light (Figure 7A; Supplemental Figure 8). It is plausible that the osmolytes normally deriving from starch degradation were replaced by the high photosynthetic sugar production in the mesophyll, which, in concomitance with K^+ uptake and inhibition of anion channels (Marten et al., 2008), was sufficient to promote rapid guard cell turgor and stomatal opening. The fact that the *aha1* mutant had reduced and slow g_s responses under these saturating light intensities (Figures 7A and 7C) led us to conclude that the activity of the PM H^+-ATPase is necessary to promote the uptake of K^+ and/or mesophyll-derived sugars for stomatal opening.

Our discovery of the slow g_s kinetics and reduced amplitude of *aha1* stomata under RL illumination (Figure 8A; Supplemental

Figure 9), which eliminates the BL-dependent response, further defines an essential role for PM H^+-ATPase in photosynthesis-mediated stomatal responses. This finding is in line with recent studies reporting that RL induces photosynthesis-dependent phosphorylation of PM H^+-ATPase in guard cells to promote stomatal opening in whole leaves (Ando and Kinoshita, 2018).

The RL response is partially driven by the accumulation of photosynthetically derived sugars, synthesized by the guard cell itself or imported from the mesophyll (Poffenroth et al., 1992; Talbott and Zeiger, 1993; Lu et al., 1995; Olsen et al., 2002), and is associated with net guard cell starch accumulation (Tallman and Zeiger, 1988; Horrer et al., 2016). It was indeed demonstrated that RL can stimulate stomatal opening via K^+ accumulation and starch breakdown (i.e., the classic BL-dependent response) only under low CO_2 conditions, when photosynthetic rates are low (Olsen et al., 2002). Because guard cell photosynthesis can provide only limited amounts of carbon (Tarczynski et al., 1989; Reckmann et al., 1990), mesophyll-derived sugars have long been considered as the most important source of osmotica for RL-mediated stomatal opening (reviewed in Lawson et al., 2014). In this study, we provide evidence supporting the role of mesophyll sugars in the RL response. When illuminated with 300 μmol m^{-2} s^{-1} of RL, guard cells in isolated epidermal peels accumulated only ~25% of starch amounts compared with guard cells of intact leaves (Figures 8C and 8D). Furthermore, stomata of intact leaves efficiently opened in response to RL, whereas isolated stomata remained closed (Figures 8E and 8F).

Early biochemical studies suggested that Suc produced by mesophyll photosynthesis is transported to the guard cells via the apoplast and is taken up into the guard cells, apparently in symport with protons (Dittrich and Raschke, 1977; Lu et al., 1997; Ritte et al., 1999). In agreement with this hypothesis, we showed that guard cells of wild-type and *aha1* plants contained different amounts of soluble sugars at the EoN, with wild-type plants showing elevated contents for all three sugars (Figures 8I and 8J; Supplemental Table 4). After the plants have been exposed to RL (300 μmol m^{-2} s^{-1}) for 2 h, this difference became more pronounced, especially for Suc. Wild-type guard cells doubled their Suc content, whereas *aha1* guard cells failed to increase Suc levels (Figure 8I; Supplemental Table 4). This, together with the fact that *aha1* mutant guard cells did not accumulate starch in response to RL irradiation (Figure 8B), lead us to conclude that the activity of H^+-ATPase under RL or saturating photosynthetic active radiation is essential to energize Suc uptake for guard cell turgor generation and starch biosynthesis. Our results are in line with research demonstrating a role for the PM H^+-ATPase (PHA1; AHA1 from potato [*Solanum tuberosum*]) in Suc-starch metabolism in stolons of potato (Stritzler et al., 2017). It is conceivable that RL-induced CO_2 fixation provides the precursors needed for starch synthesis, but whether or not this accumulation of starch is required for RL stomatal responses remains unclear.

METHODS

Plant Material and Growth Conditions

All experiments were performed with four-week–old, non-flowering Arabidopsis (*Arabidopsis thaliana*) plants in the Columbia (Col-0) background. The Arabidopsis mutants used in this study, *aha1-8* (Salk_118350C) and *amy3 bam1*, were described by Horrer et al. (2016). Plants were grown in

soil in controlled-climate chambers (either KKD Hiross from CLITEC, or a Fitoclima 1200 or Fitoclima 2500 from Aralab) under a 12-h light/12-h dark photoperiod at a constant temperature of 21°C/19°C (day/night) and a relative humidity of 45/55% (day/night). Plants were illuminated with a total photon flux density of 150 μmol m^{-2} s^{-1} with a combination of white (Biolux; Osram) and purple (Fluora; Osram) halogen lamps. Alternatively, plants were illuminated with a Fitoclima 2500 light-emitting diode (LED) panel (Aralab) or Fitoclima 2500 LED tubes (Aralab). Guard cell starch quantification and gas exchange measurements were performed at the indicated time points on plants subjected to a two-pulsed–light treatment. In a typical experimental setup, plants were given pulses of light and darkness of 2 h each. Alternatively, plants were subjected to modified versions of the two-pulsed–light treatment, in which the first light pulse or the first dark pulse were extended to 3 h. In all cases, the experiment started at the EoN when plants were directly transferred from the climate chamber to the whole-plant Arabidopsis chamber, a model no. 6400-17 (LI-COR Biosciences), and given 30 min of dark adaptation before the beginning of the first light pulse. Plants were illuminated with standard growth light conditions (150 μmol m^{-2} s^{-1}) or saturating photosynthetic active radiation (400 μmol m^{-2} s^{-1}). For the RL experiments, plants were transferred at the EoN from the climate chamber to a reach-in climate chamber equipped with LED light sources (Fytoscope FS130; Photon Systems Instruments) and illuminated with 300 μmol m^{-2} s^{-1} RL.

Guard Cell Starch Quantification

Guard cell starch content was quantified as described by Flütsch et al. (2018). In brief, at the indicated time points, epidermal peels obtained from leaf number 5 or 6 were fixed immediately in fixative solution (50% [v/v] methanol and 10% [v/v] acetic acid). Alternatively, leaves number 5 and 6 from eight individual plants were blended using a kitchen blender (ProBlend Avance, Philips). Isolated guard cells were collected using a 200-μm nylon mesh (Sefar) and incubated in 1 mL of basic opening buffer (5 mM of MES-bistrispropane at pH 6.5, 50 mM of KCl, and 0.1 mM of CaCl$_2$). Isolated guard cells were dark-incubated for 1 h in a reach-in climate chamber (model no. Fytoscope FS130; Photon Systems Instruments). The isolated guard cells were subsequently exposed to 300 μmol m^{-2} s^{-1} RL for 6 h. In a modified version of this experiment, isolated guard cells were treated with 10 μM of Fc (Sigma-Aldrich) after 3 h of RL illumination. After the incubation and at the indicated time points, isolated guard cells were fixed in 50% (v/v) methanol and 10% (v/v) acetic acid. After fixation, starch granules were stained using the modified pseudo-Schiff propidium iodide staining (Truernit et al., 2008; Flütsch et al., 2018). To oxidize the hydroxyl groups of the Glc entities, samples were incubated in 1% (w/v) periodic acid solution. The epidermal peels were stained with propidium iodide (1 mg mL^{-1} [w/v]) and Schiff reagent (100 mM of sodium metabisulphite and 5 N of HCl). After destaining in distilled water, the samples were covered with chloral hydrate solution on a microscopy slide. Finally, epidermal peels were fixed with Hoyer's solution after an overnight dark incubation. Guard cell starch contents were visualized using a model no. TCS SP5 confocal laser-scanning microscope (Leica Microsystems). Starch granule area was determined using the software ImageJ v1.48 (NIH; http://rsbweb.nih.gov/ij/).

Stomatal Aperture and Trait Analysis

Stomatal morphological parameters (aperture, guard cell length, guard cell width, and stomatal density) were measured from the fifth or the sixth leaf after 2 h of light, when stomata are fully open, as previously described by Horrer et al. (2016). For the time course of stomatal aperture, images were taken at the indicated time points. Briefly, leaf number 5 or 6 was fixed on an adhesive tape with the abaxial epidermis facing the tape. The mesophyll cell layer and the adaxial epidermis were removed using a razor blade. The abaxial epidermal cell layer remaining on the tape was washed with

a 10-mM MES-KOH, pH 6.15 solution and subsequently fixed on a microscopy slide. Stomata were immediately imaged using an inverted microscope (Eclipse TS100; Nikon) at 40× magnification.

Alternatively, isolated guard cells from leaves number 5 and 6 obtained as described in "Guard Cell Starch Quantification" were transferred to microscopy slides at the indicated time points with or without treatment with 10 μM of Fc (Sigma-Aldrich), and immediately imaged.

Stomatal anatomical traits were determined using the software ImageJ v1.48 (NIH).

Anatomical g_{smax} Calculation

The anatomical g_{smax} to water vapor (mol m^{-2} s^{-1}) was determined according to the double end-corrected version of the equation by Franks and Farquhar (2001):

$$g_{smax} = \frac{d_w S_D a_{max}}{v \left(l + \frac{\pi}{2} \sqrt{\frac{a_{max}}{\pi}} \right)}$$

where d_w is the diffusivity of water vapor in air (m^2 s^{-1}) at 22°C, v is the molar volume of air (m^3 mol^{-1}) at 1 atm and 22°C, S_D is the stomatal density (m^{-2}), and l represents the guard cell pore depth (m).

Maximum stomatal pore area (a_{max}) was calculated as $\pi \left(\frac{p}{2} \right)^2$. The maximum stomatal pore area was an ellipse with the main axis equal to pore length L (m) and the minor axis equal to $L/2$.

GCP Isolation and H$^+$ Pumping

GCPs were enzymatically prepared from Arabidopsis wild-type or *amy3 bam1* mutant leaves as described previously by Yamauchi and Shimazaki (2017). Isolated, overnight dark-adapted GCPs were illuminated with 50 μmol m^{-2} s^{-1} of RL for 2 h, after which BL (10 μmol m^{-2} s^{-1}) was applied for 30 min. BL-dependent H$^+$-extrusion was determined using a glass pH-electrode as described by Yamauchi and Shimazaki (2017). The reaction mixture (0.8 mL) was composed of 0.125 mM of MES-KOH at pH 6.0, 10 mM of KCl, 0.4 M of mannitol, 1 mM of CaCl$_2$, and Arabidopsis GCPs (50 to 80 μg of protein).

Determination of Phosphorylation Levels of PM H$^+$-ATPase

GCPs were exposed to 50 μmol m^{-2} s^{-1} of RL for 30 min, after which BL (10 μmol m^{-2} s^{-1}) was applied. Immunoblotting was performed as previously described by Kinoshita and Shimazaki (1999) with slight modifications. The antibodies against the H$^+$-ATPase were reported by Kinoshita and Shimazaki (1999). The phospho-specific antibodies against the penultimate Thr of H$^+$-ATPase (anti-pThr) were raised in rabbits according to Hayashi et al. (2010).

Measurements of K$^+$ Currents

Currents were recorded using double-barreled microelectrodes as described by Chen et al. (2012) using Henry's EP software (http://www.psrg.org.uk). To record inwardly rectifying K$^+$ currents ($I_{K,in}$) and outwardly rectifying K$^+$ currents ($I_{K,out}$), electrodes were filled with 200 mM of K-acetate at pH 7.5 to avoid anion leakage from the microelectrode (Blatt and Slayman, 1983; Chen et al., 2012). Microelectrodes were constructed to give tip resistances >500 MΩ for Arabidopsis guard cell impalements. Guard cells from epidermal peels were treated with depolarizing buffer and light of 150 μmol m^{-2} s^{-1} before recording K$^+$ currents in standard bathing solution of 5 mM of Ca^{2+}-MES at pH 6.1 containing 10 mM of KCl. Voltage and currents were recorded using a μP electrometer amplifier (WyeScience) with an input impedance of >2·10^{11} Ω (Blatt, 1987). Surface area

and volume of impaled guard cells were estimated from the cell length and diameter, assuming a spheroid geometry.

Measurements of Cl^- Currents

Voltage-clamp recordings were performed from Arabidopsis intact guard cells in epidermal peels using Henry's EP Software Suite (http://www.psrg.org.uk). Double-barreled microelectrodes were filled with 200 mM of CsCl at pH 7.5, and the tissue was superfused with 5 mM of MES-Ca^{2+} at pH 6.1, containing 15 mM of CsCl and 15 mM of tetraethylammonium chloride. Surface areas of impaled guard cells were calculated assuming a spheroid geometry (Blatt and Slayman, 1983) and voltages were analyzed using Henry's EP Software Suite. For clarity, the data of instantaneous current were fitted with a second-order polynomial function: $I = y_0 + ax + bx^2$.

Gas Exchange Measurements

Whole-plant gas exchange measurements were performed using a model no. 6400 XT Infrared Gas Analyzer equipped with a 6400-18 light source and the whole-plant Arabidopsis 6400-17 chamber (all from LI-COR Biosciences). To prevent any CO_2 diffusion and water vapor from the soil, the pots were sealed with a clear film. All measurements were performed at 22°C, 50% relative humidity, and 400 μg mL^{-1} CO_2. Before measurements, plants were equilibrated in darkness for 30 min. Measurements of net A and g_s values were performed on at least three different plants per genotype and light treatment, starting always at the same time of the diurnal cycle (EoN). Whole rosette area was determined using the software ImageJ v1.48 (NIH). The g_s and A values were normalized by subtracting the conductance values EoN (set as 0 = initial values for g_s or A) as described by Baroli et al. (2008). In all experiments, normalized g_s values during the dark pulses were lower compared with the g_s values at time 0 due to stomatal preopening during the last hours of the night period (Lebaudy et al., 2008). Calculation of gas- exchange parameters were made, according to von Caemmerer and Farquhar (1981) with C_i corrected for water vapor efflux from the leaf.

Temporal Response of g_s

The temporal response of g_s to light has been described by a time constant (τ) estimated using an exponential equation:

$$g_s = g_{max} + (g_{min} - g_{max})e^{-t/\tau} \qquad (1)$$

with g_{min} and g_{max} being the minimum and maximum g_s. The time constant represents the time to reach 63% of the total g_s variation, and was used to estimate the maximum slope (Sl_{max}) using the maximum derivative:

$$Sl_{max} = \frac{g_{max} - g_{min}}{\tau} \qquad (2)$$

Equation 1 was fitted on the observed data of each genotype collected in the different experiments using a non-linear mixed effect model. Fixed effects were set for g_{min}, g_{max}, and τ, and random effect were set for g_{min} and g_{max}. The average and confidence interval estimated with this model was calculated for each genotype and experimental conditions. The analysis was performed using the R (v3.4.1) package nlme (v3.1) and the nlme function. Initial parameter values were approximated using the initial and final g_s observed, and the time to reach 63% of the observed variation for τ.

RNA Isolation and Quantitative PCR Analysis

For RNA extraction from leaf material, three entire rosettes per genotype and time point (three biological replicates) were harvested and frozen in liquid nitrogen.

For RNA extraction from epidermal peels, the middle veins of 12 rosettes per genotype and time point (one biological replicate) were excised and the remaining leaf material was blended in 100 mL of ice-cold water using a blender (ProBlend Avance, Philips). A total of three biological replicates per genotype and time point were used for one experiment. The blended material was passed through a 200-μm nylon mesh (Sefar) and the remaining epidermal peels were dried, collected, and immediately frozen in liquid nitrogen. Subsequently, the epidermal peels were ground using a tissue grinder (Mix Mill MM-301; Retsch). Total RNA was extracted from 30 mg of ground tissue using the SV Total RNA Isolation Kit (Promega) following the manufacturer's instructions. RNA quality and quantity were determined with a NanoDrop ND-1000 spectrophotometer (Thermo Fisher Scientific). A total of 1 μg of RNA was used for cDNA first-strand synthesis using the M-MLV Reverse Transcriptase RNase H Minus Point Mutant and oligo(dT)$_{15}$ primer (Promega). Transcript levels were examined by RT-qPCR using the SYBR Green Master Mix (Applied Biosystems) and the 7500 Fast Real-Time PCR System (Applied Biosystems). RT-qPCR was performed in triplicates. Transcript levels were calculated according to the comparative C_T method (Livak and Schmittgen, 2001) and were normalized against the expression of the *Actin2* gene (*ACT2*; At3g18780). Error calculations were done according to Applied Biosystems guidelines (http://www3.appliedbiosystems.com/cms/groups/mcb_support /documents/generaldocuments/cms_042380.pdf). Primers and PCR efficiencies for RT-qPCR are listed in Supplemental Table 5.

Mesophyll Starch Extraction and Quantification

Mesophyll starch contents were determined enzymatically according to Hostettler et al. (2011). In brief, entire Arabidopsis rosettes were harvested at the indicated time points and immediately frozen in liquid nitrogen. Rosettes were homogenized using a tissue grinder (Mix Mill MM-301; Retsch) and resuspended in 0.7M perchloric acid. Insoluble material was washed three times with 70% (v/v) ethanol and subsequently resuspended in water. Starch was solubilized by heating (95°C) and thereafter digested to Glc via enzymatic reactions (α-amylase and amyloglucosidase, both from Roche) at 37°C. The amount of Glc equivalents was determined using the enzymes hexokinase (Roche) and Glc-6-phosphate dehydrogenase (Roche), which convert NAD to NADH in an equimolar ratio. The increase in NADH was determined spectrophotometrically (Synergy H1; BioTek) by monitoring the absorption spectrum at 340 nm.

Guard Cell Soluble Sugar Quantification

To extract soluble sugars from guard-cell–enriched epidermal peels, six rosettes per genotype, corresponding to one biological replicate, were collected at the EoN or after the plants were exposed to 300 μmol m^{-2} s^{-1} of RL for 2 h, and the petiole was removed using scissors. The remaining leaf material was blended in 100 mL of ice-cold water using a kitchen blender (Avance Collection, Philips). The blended material was filtered through a 200-μm nylon mesh and the remaining epidermal peels were dried, collected in a tube, and immediately frozen in liquid nitrogen. Alternatively, epidermal peels from EoN samples were collected from the nylon mesh and incubated in basic opening buffer (5 mM of MES-bistrispropane at pH 6.5, 50 mM of KCl, and 0.1 mM of CaCl$_2$) for 30 min under 75 μmol m^{-2} s^{-1} of BL or darkness.

To remove residual sugars from the guard cell apoplast, the samples were washed with 2 L of Milli-Q water (Merck Millipore) according to Daloso et al. (2015) and refrozen in liquid nitrogen. Subsequently, guard-cell–enriched epidermal peel materials were ground into a fine powder with a ball mill (Mix Mill MM-301; Retsch). Up to six biological replicates per genotype and time point were harvested for one experiment. Two independent experiments were performed.

Soluble sugars were extracted as described by Thalmann et al. (2016). After the extraction, the samples were lyophilized in a freeze-dryer (Lyovac GT1; Lybold) and resuspended in 60 µL of Milli-Q water (Merck Millipore).

Guard cell soluble sugars were quantified based on the protocol for quantification of root soluble sugars described by Thalmann et al. (2016) using 50 µL of neutralized soluble fraction obtained from the lyophilized and resuspended initial perchloric acid extraction as starting material.

Leaf Soluble Sugar Quantification

Leaf soluble sugars were determined enzymatically according to Thalmann et al. (2016). In brief, entire Arabidopsis rosettes were harvested at the EoN and immediately frozen in liquid nitrogen. Rosettes were homogenized using a tissue grinder (Mix Mill MM-301; Retsch) and resuspended in 0.7 M perchloric acid. After pelleting the insoluble material, 600 µL of clear supernatant was transferred to a fresh 1.5-mL Eppendorf tube. The soluble fraction was neutralized with neutralization buffer (400 mM of MES and 2 M of KOH), and 600 µL of clear supernatant was kept for analysis. Eight rosettes per genotype were harvested for one experiment. Soluble sugars were quantified using 20 µL of neutralized soluble fraction obtained from the initial perchloric acid extraction.

Guard Cell Malate Quantification

To quantify the amount of malate from guard-cell–enriched epidermal peels, six rosettes per genotype, corresponding to one biological replicate, were collected at the EoN and the leaf material was blended in 100 mL of ice-cold water using a kitchen blender (Avance Collection, Philips). The blended material was filtered through a 200-µm nylon mesh and either dried, collected, and immediately frozen in liquid nitrogen, or incubated in basic opening buffer (5 mM of MES-bistrispropane at pH 6.5, 50 mM of KCl, and 0.1 mM of $CaCl_2$) for 30 min under 75 µmol m^{-2} s^{-1} of BL or darkness.

The samples were washed extensively with 2 L of Milli-Q water to remove residual organic acids from the guard cell apoplast according to Daloso et al. (2015). Afterwards, guard-cell–enriched epidermal peel materials were ground into a fine powder with a ball mill (Mix Mill MM-301; Retsch). Up to six biological replicates per genotype and time point were harvested for one experiment. Two independent experiments were performed.

To extract organic acids, 1 mL of Milli-Q water was added to the ground tissues and the samples were incubated at 95°C for 15 min, followed by 10 min of centrifugation at 16,000 g to collect the supernatant. After the extraction, samples were lyophilized in a Lyovac GT1 freeze-dryer (Lybold) and resuspended in 60 µL of Milli-Q water.

L-malate content was determined using the K-LMAL-116A kit (Megazyme) following the manufacturer's protocol using 50 µL of the lyophilized and resuspended organic acid extract.

Malate Quantification in Leaves

Malate content of leaves was determined using the K-LMAL-116A kit (Megazyme) following the manufacturer's protocol. Entire Arabidopsis rosettes were harvested at the EoN and immediately frozen in liquid nitrogen. Malate was extracted as described above in "Guard Cell Malate Quantification." Eight rosettes per genotype were harvested for one experiment. L-malate content was determined using 10 µL of the initial organic acid extract.

Statistical Analysis

Statistical differences between genotypes and time points were determined by ANOVA with post hoc Tukey's Honest Significant Difference test (P-value < 0.05) or by the unpaired Student's t test. Statistical significance was marked as follows: *$P < 0.05$; **$P < 0.01$; ***$P < 0.001$. All data are indicated as means ± SE. Details are given in Supplemental File 2.

Accession Numbers

Sequence data from this article can be found in the Arabidopsis Genome Initiative or GenBank/EMBL databases under the following accession numbers: At3g23920 (*BAM1*), At1g69830 (*AMY3*), and At2g18960 (*AHA1*).

Supplemental Data

Supplemental Figure 1. Quantification of H$^+$-ATPase phosphorylation levels and g_s kinetics under BL illumination superimposed on RL (supports Figure 1).

Supplemental Figure 2. Metabolite quantification in guard cells and leaves under darkness (supports Figure 2).

Supplemental Figure 3. Stomatal opening responses of wild-type, *amy3 bam1*, and *aha1* plants subjected to a two-pulsed–light treatment (supports Figure 3).

Supplemental Figure 4. Gene expression of *AHA2* and *AHA5* in guard cells of *aha1* mutant (supports Figure 3).

Supplemental Figure 5. Leaf starch content of plants subjected to a two-pulsed–light treatment (supports Figure 3).

Supplemental Figure 6. Stomatal opening responses of wild-type, *amy3 bam1*, and *aha1* plants subjected to a modified two-pulsed–light treatment (supports Figure 4).

Supplemental Figure 7. Effect of time of day on wild-type stomatal kinetics and photosynthesis (supports Figure 5).

Supplemental Figure 8. Stomatal opening responses of wild-type, *amy3 bam1*, and *aha1* plants subjected to a two-pulsed–light treatment under saturating photosynthetic active radiation (supports Figure 7)

Supplemental Figure 9. Stomatal opening responses of wild-type, *amy3 bam1*, and *aha1* plants in response to RL (supports Figure 8).

Supplemental Table 1. Malate content of guard-cell–enriched epidermal peels of the wild type and *amy3 bam1* treated with BL (supports Figure 2).

Supplemental Table 2. Soluble sugar content of guard-cell–enriched epidermal peels of the wild type and *amy3bam1* treated with BL (supports Figure 2).

Supplemental Table 3. Temporal responses of g_s in the wild type, *amy3 bam1*, and *aha1* subject to different two-pulsed–light treatments (supports Figure 3).

Supplemental Table 4. Soluble sugar content of guard-cell–enriched epidermal peels of the wild type and *aha1* treated with RL (supports Figure 4).

Supplemental Table 5. Sequences of primers used for RT-qPCR (supports Supplemental Figure 4).

Supplemental File 1. Estimation of H$^+$ extrusion rate in intact guard cells of Arabidopsis (supports Figure 1).

Supplemental File 2. Statistical analysis.

AUTHOR CONTRIBUTIONS

D.S., M.R.B., and S.F. designed the research; S.F., Y.W., A.T., S.R.M.V.-C., M.K., and A.N. performed the research; A.H. added software utilities for data analysis; S.F., T.L., M.R.B., and D.S. analyzed the data; D.S., S.F., T.L., and M.R.B. wrote the article with approval from all authors.

REFERENCES

Allaway, W.G. (1973). Accumulation of malate in guard cells of *Vicia faba* during stomatal opening. Planta **110:** 63–70.

Amodeo, G., Talbott, L.D., and Zeiger, E. (1996). Use of potassium and sucrose by onion guard cells during a daily cycle of osmoregulation. Plant Cell Physiol. **37:** 575–579.

Ando, E., and Kinoshita, T. (2018). Red light-induced phosphorylation of plasma membrane H$^+$-ATPase in stomatal guard cells. Plant Physiol. **178:** 838–849.

Asai, N., Nakajima, N., Tamaoki, M., Kamada, H., and Kondo, N. (2000). Role of malate synthesis mediated by phosphoenolpyruvate carboxylase in guard cells in the regulation of stomatal movement. Plant Cell Physiol. **41:** 10–15.

Assmann, S.M., Simoncini, L., and Schroeder, J.I. (1985). Blue light activates electrogenic ion pumping in guard cell protoplasts of *Vicia faba*. Nature **318:** 285–287.

Baroli, I., Price, G.D., Badger, M.R., and von Caemmerer, S. (2008). The contribution of photosynthesis to the red light response of stomatal conductance. Plant Physiol. **146:** 737–747.

Barradas, V.L., and Jones, H.G. (1996). Responses of CO_2 assimilation to changes in irradiance: Laboratory and field data and a model for beans (*Phaseolus vulgaris* L.). J. Exp. Bot. **47:** 639–645.

Berry, J.A., Beerling, D.J., and Franks, P.J. (2010). Stomata: Key players in the earth system, past and present. Curr. Opin. Plant Biol. **13:** 233–240.

Blatt, M.R. (1987). Electrical characteristics of stomatal guard cells: the contribution of ATP-dependent, "electrogenic" transport revealed by current-voltage and difference-current-voltage analysis. J. Membr. Biol. **98:** 257–274.

Blatt, M.R. (2016). Plant physiology: Redefining the enigma of metabolism in stomatal movement. Curr. Biol. **26:** R107–R109.

Blatt, M.R., and Slayman, C.L. (1983). KCl leakage from microelectrodes and its impact on the membrane parameters of a non-excitable cell. J. Membr. Biol. **72:** 223–234.

Büssis, D., Von Groll, U., Fisahn, J., and Altmann, T. (2006). Stomatal aperture can compensate altered stomatal density in *Arabidopsis thaliana* at growth light conditions. Funct. Plant Biol. **33:** 1037–1043.

Chen, Z.-H., Eisenach, C., Xu, X.-Q., Hills, A., and Blatt, M.R. (2012). Protocol: Optimised electrophysiological analysis of intact guard cells from Arabidopsis. Plant Methods **8:** 15.

Daloso, D.M., Antunes, W.C., Pinheiro, D.P., Waquim, J.P., Araújo, W.L., Loureiro, M.E., Fernie, A.R., and Williams, T.C.R. (2015). Tobacco guard cells fix CO_2 by both Rubisco and PEPcase while sucrose acts as a substrate during light-induced stomatal opening. Plant Cell Environ. **38:** 2353–2371.

Daloso, D.M., Dos Anjos, L., and Fernie, A.R. (2016). Roles of sucrose in guard cell regulation. New Phytol. **211:** 809–818.

Daloso, D.M., Medeiros, D.B., Dos Anjos, L., Yoshida, T., Araújo, W.L., and Fernie, A.R. (2017). Metabolism within the specialized guard cells of plants. New Phytol. **216:** 1018–1033.

Dittrich, P., and Raschke, K. (1977). Uptake and metabolism of carbohydrates by epidermal tissue. Planta **134:** 83–90.

Dow, G.J., Bergmann, D.C., and Berry, J.A. (2014). An integrated model of stomatal development and leaf physiology. New Phytol. **201:** 1218–1226.

Drake, P.L., Froend, R.H., and Franks, P.J. (2013). Smaller, faster stomata: Scaling of stomatal size, rate of response, and stomatal conductance. J. Exp. Bot. **64:** 495–505.

Elliott-Kingston, C., Haworth, M., Yearsley, J.M., Batke, S.P., Lawson, T., and McElwain, J.C. (2016). Does size matter? Atmospheric CO_2 may be a stronger driver of stomatal closing rate than stomatal size in taxa that diversified under low CO_2. Front Plant Sci **7:** 1253.

Fischer, R.A. (1968). Stomatal opening: Role of potassium uptake by guard cells. Science **160:** 784–785.

Fischer, R.A., and Hsiao, T.C. (1968). Stomatal opening in isolated epidermal strips of *Vicia faba*. II. Responses to KCl concentrations and the role of potassium absorption. Plant Physiol. **43:** 1953–1958.

Flütsch, S., Distefano, L., and Santelia, D. (2018). Quantification of starch in guard cells of *Arabidopsis thaliana*. Bio Protoc. **8:** e2920.

Franks, P.J., and Beerling, D.J. (2009). Maximum leaf conductance driven by CO_2 effects on stomatal size and density over geologic time. Proc. Natl. Acad. Sci. USA **106:** 10343–10347.

Franks, P.J., and Farquhar, G.D. (2001). The effect of exogenous abscisic acid on stomatal development, stomatal mechanics, and leaf gas exchange in *Tradescantia virginiana*. Plant Physiol. **125:** 935–942.

Franks, P.J., and Farquhar, G.D. (2007). The mechanical diversity of stomata and its significance in gas-exchange control. Plant Physiol. **143:** 78–87.

George, G.M., Kölling, K., Kuenzli, R., Hirsch-Hoffmann, M., Flütsch, P., and Zeeman, S.C. (2018). Design and use of a digitally controlled device for accurate, multiplexed gas exchange measurements of the complete foliar parts of plants. Methods Mol. Biol. **1770:** 45–68.

Granot, D., and Kelly, G. (2019). Evolution of guard-cell theories: The story of sugars. Trends Plant Sci. **24:** 507–518.

Haworth, M., Elliott-Kingston, C., and McElwain, J.C. (2011). Stomatal control as a driver of plant evolution. J. Exp. Bot. **62:** 2419–2423.

Hayashi, Y., Nakamura, S., Takemiya, A., Takahashi, Y., Shimazaki, K., and Kinoshita, T. (2010). Biochemical characterization of *in vitro* phosphorylation and dephosphorylation of the plasma membrane H$^+$-ATPase. Plant Cell Physiol. **51:** 1186–1196.

Hetherington, A.M., and Woodward, F.I. (2003). The role of stomata in sensing and driving environmental change. Nature **424:** 901–908.

Hiyama, A., Takemiya, A., Munemasa, S., Okuma, E., Sugiyama, N., Tada, Y., Murata, Y., and Shimazaki, K.I. (2017). Blue light and CO_2 signals converge to regulate light-induced stomatal opening. Nat. Commun. **8:** 1284.

Horrer, D., Flütsch, S., Pazmino, D., Matthews, J.S.A., Thalmann, M., Nigro, A., Leonhardt, N., Lawson, T., and Santelia, D. (2016). Blue light induces a distinct starch degradation pathway in guard cells for stomatal opening. Curr. Biol. **26:** 362–370.

Hostettler, C., Kölling, K., Santelia, D., Streb, S., Kötting, O., and Zeeman, S.C. (2011). Analysis of starch metabolism in chloroplasts. Methods Mol. Biol. **775:** 387–410.

Humble, G.D., and Raschke, K. (1971). Stomatal opening quantitatively related to potassium transport: Evidence from electron probe analysis. Plant Physiol. **48:** 447–453.

Inoue, S.I., and Kinoshita, T. (2017). Blue light regulation of stomatal opening and the plasma membrane H^+-ATPase. Plant Physiol. **174:** 531–538.

Jezek, M., and Blatt, M.R. (2017). The membrane transport system of the guard cell and its integration for stomatal dynamics. Plant Physiol. **174:** 487–519.

Kinoshita, T., and Shimazaki, K. (1999). Blue light activates the plasma membrane H^+-ATPase by phosphorylation of the C-terminus in stomatal guard cells. EMBO J. **18:** 5548–5558.

Lawson, T., and Blatt, M.R. (2014). Stomatal size, speed, and responsiveness impact on photosynthesis and water use efficiency. Plant Physiol. **164:** 1556–1570.

Lawson, T., Lefebvre, S., Baker, N.R., Morison, J.I.L., and Raines, C.A. (2008). Reductions in mesophyll and guard cell photosynthesis impact on the control of stomatal responses to light and CO_2. J. Exp. Bot. **59:** 3609–3619.

Lawson, T., Simkin, A.J., Kelly, G., and Granot, D. (2014). Mesophyll photosynthesis and guard cell metabolism impacts on stomatal behaviour. New Phytol. **203:** 1064–1081.

Lawson, T., and Vialet-Chabrand, S. (2019). Speedy stomata, photosynthesis and plant water use efficiency. New Phytol. **221:** 93–98.

Lebaudy, A., Vavasseur, A., Hosy, E., Dreyer, I., Leonhardt, N., Thibaud, J.-B., Véry, A.-A., Simonneau, T., and Sentenac, H. (2008). Plant adaptation to fluctuating environment and biomass production are strongly dependent on guard cell potassium channels. Proc. Natl. Acad. Sci. USA **105:** 5271–5276.

Lee, J.S., and Bowling, D.J.F. (1992). Influence of the mesophyll on stomatal opening in *Commelina communis*. J. Exp. Bot. **43:** 951–957.

Lee, M., Choi, Y., Burla, B., Kim, Y.-Y., Jeon, B., Maeshima, M., Yoo, J.-Y., Martinoia, E., and Lee, Y. (2008). The ABC transporter AtABCB14 is a malate importer and modulates stomatal response to CO_2. Nat. Cell Biol. **10:** 1217–1223.

Lima, V.F., Medeiros, D.B., Dos Anjos, L., Gago, J., Fernie, A.R., and Daloso, D.M. (2018). Toward multifaceted roles of sucrose in the regulation of stomatal movement. Plant Signal. Behav. **13:** e1494468.

Livak, K.J., and Schmittgen, T.D. (2001). Analysis of relative gene expression data using real-time quantitative PCR and the $2^{-\Delta\Delta C(T)}$ Method. Methods **25:** 402–408.

Lloyd, F. (1908). The behaviour of stomata. Carnegie Inst. Wash. Publ. **82:** 1–142.

Lu, P., Outlaw, W.H., Jr., Smith, B.G., and Freed, G.A. (1997). A new mechanism for the regulation of stomatal aperture size in intact leaves. Plant Physiol. **114:** 109–118.

Lu, P., Zhang, S.Q., Outlaw, W.H., Jr., and Riddle, K.A. (1995). Sucrose: A solute that accumulates in the guard-cell apoplast and guard-cell symplast of open stomata. FEBS Lett. **362:** 180–184.

Marten, H., Hedrich, R., and Roelfsema, M.R.G. (2007). Blue light inhibits guard cell plasma membrane anion channels in a phototropin-dependent manner. Plant J. **50:** 29–39.

Marten, H., Hyun, T., Gomi, K., Seo, S., Hedrich, R., and Roelfsema, M.R.G. (2008). Silencing of NtMPK4 impairs CO-induced stomatal closure, activation of anion channels and cytosolic Ca^{2+} signals in *Nicotiana tabacum* guard cells. Plant J. **55:** 698–708.

Matrosova, A., Bogireddi, H., Mateo-Peñas, A., Hashimoto-Sugimoto, M., Iba, K., Schroeder, J.I., and Israelsson-Nordström, M. (2015). The HT1 protein kinase is essential for red light-induced stomatal opening and genetically interacts with OST1 in red light and CO_2-induced stomatal movement responses. New Phytol. **208:** 1126–1137.

McAusland, L., Vialet-Chabrand, S., Davey, P., Baker, N.R., Brendel, O., and Lawson, T. (2016). Effects of kinetics of light-induced stomatal responses on photosynthesis and water-use efficiency. New Phytol. **211:** 1209–1220.

McLachlan, D.H., Lan, J., Geilfus, C.M., Dodd, A.N., Larson, T., Baker, A., Hõrak, H., Kollist, H., He, Z., Graham, I., Mickelbart, M.V., and Hetherington, A.M. (2016). The breakdown of stored triacylglycerols is required during light-induced stomatal opening. Curr. Biol. **26:** 707–712.

Medeiros, D.B., Perez Souza, L., Antunes, W.C., Araújo, W.L., Daloso, D.M., and Fernie, A.R. (2018). Sucrose breakdown within guard cells provides substrates for glycolysis and glutamine biosynthesis during light-induced stomatal opening. Plant J. **94:** 583–594.

Messinger, S.M., Buckley, T.N., and Mott, K.A. (2006). Evidence for involvement of photosynthetic processes in the stomatal response to CO_2. Plant Physiol. **140:** 771–778.

Mott, K.A., Sibbernsen, E.D., and Shope, J.C. (2008). The role of the mesophyll in stomatal responses to light and CO_2. Plant Cell Environ. **31:** 1299–1306.

Murata, Y., Mori, I.C., and Munemasa, S. (2015). Diverse stomatal signaling and the signal integration mechanism. Annu. Rev. Plant Biol. **66:** 369–392.

Naumburg, E., Ellsworth, D.S., and Katul, G.G. (2001). Modeling dynamic understory photosynthesis of contrasting species in ambient and elevated carbon dioxide. Oecologia **126:** 487–499.

Olsen, R.L., Pratt, R.B., Gump, P., Kemper, A., and Tallman, G. (2002). Red light activates a chloroplast-dependent ion uptake mechanism for stomatal opening under reduced CO_2 concentrations in *Vicia* spp. New Phytol. **153:** 497–508.

Ooba, M., and Takahashi, H. (2003). Effect of asymmetric stomatal response on gas-exchange dynamics. Ecol. Modell. **164:** 65–82.

Outlaw, W.H., and Lowry, O.H. (1977). Organic acid and potassium accumulation in guard cells during stomatal opening. Proc. Natl. Acad. Sci. USA **74:** 4434–4438.

Outlaw, W.H., and Manchester, J. (1979). Guard cell starch concentration quantitatively related to stomatal aperture. Plant Physiol. **64:** 79–82.

Papanatsiou, M., Petersen, J., Henderson, L., Wang, Y., Christie, J.M., and Blatt, M.R. (2019). Optogenetic manipulation of stomatal kinetics improves carbon assimilation, water use, and growth. Science **363:** 1456–1459.

Poffenroth, M., Green, D.B., and Tallman, G. (1992). Sugar concentrations in guard cells of *Vicia faba* illuminated with red or blue light: Analysis by high performance liquid chromatography. Plant Physiol. **98:** 1460–1471.

Qu, et al. (2016). Rapid stomatal response to fluctuating light: An under-explored mechanism to improve drought tolerance in rice. Funct. Plant Biol. **43:** 727–738.

Raschke, K., and Schnabl, H. (1978). Availability of chloride affects the balance between potassium chloride and potassium malate in guard cells of *Vicia faba* L. Plant Physiol. **62:** 84–87.

Raven, J.A. (2014). Speedy small stomata? J. Exp. Bot. **65:** 1415–1424.

Reckmann, U., Scheibe, R., and Raschke, K. (1990). Rubisco activity in guard cells compared with the solute requirement for stomatal opening. Plant Physiol. **92:** 246–253.

Ritte, G., Rosenfeld, J., Rohrig, K., and Raschke, K. (1999). Rates of sugar uptake by guard cell protoplasts of *pisum sativum* L. related to the solute requirement for stomatal opening. Plant Physiol. **121:** 647–656.

Robaina-Estévez, S., Daloso, D.M., Zhang, Y., Fernie, A.R., and Nikoloski, Z. (2017). Resolving the central metabolism of Arabidopsis guard cells. Sci. Rep. **7:** 8307.

Santelia, D., and Lawson, T. (2016). Rethinking guard cell metabolism. Plant Physiol. **172:** 1371–1392.

Santelia, D., and Lunn, J.E. (2017). Transitory starch metabolism in guard cells: Unique features for a unique function. Plant Physiol. **174:** 539–549.

Scarth, G.W. (1927). Stomatal movement: Its regulation and regulatory role. A review. Protoplasma **2:** 498–511.

Schnabl, H. (1980a). CO_2 and malate metabolism in starch-containing and starch-lacking guard-cell protoplasts. Planta **149:** 52–58.

Schnabl, H. (1980b). Anion metabolism as correlated with the volume changes of guard cell protoplasts. Z. Naturforsch. C **35c:** 621–626.

Schnabl, H., Elbert, C., and Krämer, G. (1982). The regulation of the starch-malate balances during volume changes of guard cell protoplasts. J. Exp. Bot. **33:** 996–1003.

Schnabl, H., and Raschke, K. (1980). Potassium chloride as stomatal osmoticum in *Allium cepa* L., a species devoid of starch in guard cells. Plant Physiol. **65:** 88–93.

Shimazaki, K., Doi, M., Assmann, S.M., and Kinoshita, T. (2007). Light regulation of stomatal movement. Annu. Rev. Plant Biol. **58:** 219–247.

Shimazaki, K.I., Iino, M., and Zeiger, E. (1986). Blue light-dependent proton extrusion by guard cell protoplasts of *Vicia faba*. Nature **319:** 324–326.

Stritzler, M., Muñiz García, M.N., Schlesinger, M., Cortelezzi, J.I., and Capiati, D.A. (2017). The plasma membrane H^+-ATPase gene family in *Solanum tuberosum* L. role of PHA1 in tuberization. J. Exp. Bot. **68:** 4821–4837.

Suetsugu, N., Takami, T., Ebisu, Y., Watanabe, H., Iiboshi, C., Doi, M., and Shimazaki, K. (2014). Guard cell chloroplasts are essential for blue light-dependent stomatal opening in Arabidopsis. PLoS One **9:** e108374.

Talbott, L.D., and Zeiger, E. (1993). Sugar and organic acid accumulation in guard cells of *Vicia faba* in response to red and blue light. Plant Physiol. **102:** 1163–1169.

Talbott, L.D., and Zeiger, E. (1996). Central roles for potassium and sucrose in guard cell osmoregulation. Plant Physiol. **111:** 1051–1057.

Tallman, G., and Zeiger, E. (1988). Light quality and osmoregulation in *Vicia* guard cells: Evidence for involvement of three metabolic pathways. Plant Physiol. **88:** 887–895.

Tanaka, Y., Sugano, S.S., Shimada, T., and Hara-Nishimura, I. (2013). Enhancement of leaf photosynthetic capacity through increased stomatal density in Arabidopsis. New Phytol. **198:** 757–764.

Tarczynski, M.C., Outlaw, W.H., Arold, N., Neuhoff, V., and Hampp, R. (1989). Electrophoretic assay for ribulose 1,5-bisphosphate carboxylase/oxygenase in guard cells and other leaf cells of *Vicia faba* L. Plant Physiol. **89:** 1088–1093.

Thalmann, M., Pazmino, D., Seung, D., Horrer, D., Nigro, A., Meier, T., Kölling, K., Pfeifhofer, H.W., Zeeman, S.C., and Santelia, D. (2016). Regulation of leaf starch degradation by abscisic acid is important for osmotic stress tolerance in plants. Plant Cell **28:** 1860–1878.

Travis, A.J., and Mansfield, T.A. (1977). Studies of malate formation in "isolated" guard cells. New Phytol. **78:** 541–546.

Truernit, E., Bauby, H., Dubreucq, B., Grandjean, O., Runions, J., Barthélémy, J., and Palauqui, J.-C. (2008). High-resolution whole-mount imaging of three-dimensional tissue organization and gene expression enables the study of phloem development and structure in Arabidopsis. Plant Cell **20:** 1494–1503.

Ueno, K., Kinoshita, T., Inoue, S., Emi, T., and Shimazaki, K. (2005). Biochemical characterization of plasma membrane H^+-ATPase activation in guard cell protoplasts of *Arabidopsis thaliana* in response to blue light. Plant Cell Physiol. **46:** 955–963.

Vialet-Chabrand, S.R.M., Dreyer, E., and Brendel, O. (2013). Performance of a new dynamic model for predicting diurnal time courses of stomatal conductance at the leaf level. Plant Cell Environ. **36:** 1529–1546.

Vialet-Chabrand, S.R.M., Matthews, J.S.A., Brendel, O., Blatt, M.R., Wang, Y., Hills, A., Griffiths, H., Rogers, S., and Lawson, T. (2016). Modelling water use efficiency in a dynamic environment: An example using *Arabidopsis thaliana*. Plant Sci. **251:** 65–74.

Vialet-Chabrand, S.R.M., Matthews, J.S.A., McAusland, L., Blatt, M.R., Griffiths, H., and Lawson, T. (2017a). Temporal dynamics of stomatal behavior: modeling and implications for photosynthesis and water use. Plant Physiol. **174:** 603–613.

Vialet-Chabrand, S.R.M., Matthews, J.S.A., Simkin, A.J., Raines, C.A., and Lawson, T. (2017b). Importance of fluctuations in light on plant photosynthetic acclimation. Plant Physiol. **173:** 2163–2179.

Vico, G., Manzoni, S., Palmroth, S., and Katul, G. (2011). Effects of stomatal delays on the economics of leaf gas exchange under intermittent light regimes. New Phytol. **192:** 640–652.

von Caemmerer, S., and Farquhar, G.D. (1981). Some relationships between the biochemistry of photosynthesis and the gas exchange of leaves. Planta **153:** 376–387.

Wang, Y., Hills, A., Vialet-Chabrand, S., Papanatsiou, M., Griffiths, H., Rogers, S., Lawson, T., Lew, V.L., and Blatt, M.R. (2017). Unexpected connections between humidity and ion transport discovered using a model to bridge guard cell-to-leaf scales. Plant Cell **29:** 2921–2939.

Wang, Y., Papanatsiou, M., Eisenach, C., Karnik, R., Williams, M., Hills, A., Lew, V.L., and Blatt, M.R. (2012). Systems dynamic modeling of a guard cell Cl^- channel mutant uncovers an emergent homeostatic network regulating stomatal transpiration. Plant Physiol. **160:** 1956–1967.

Wong, S.C., Cowan, I.R., and Farquhar, G.D. (1979). Stomatal conductance correlates with photosynthetic capacity. Nature **282:** 424–426.

Woodrow, I.E., and Mott, K.A. (1989). Rate limitation of non-steady-state photosynthesis by ribulose-1,5-bisphosphate carboxylase in spinach. Aust. J. Plant Physiol. **16:** 487–500.

Woodrow, I.E., and Mott, K.A. (1992). Biophasic activation of ribulose bisphosphate carboxylase in spinach leaves as determined from nonsteady-state CO_2 exchange. Plant Physiol. **99:** 298–303.

Yamauchi, S., and Shimazaki, K. (2017). Determination of H^+-ATPase activity in Arabidopsis guard cell protoplasts through H^+-pumping measurement and H^+-ATPase quantification. Bio Protoc. **7.**

Yamauchi, S., Takemiya, A., Sakamoto, T., Kurata, T., Tsutsumi, T., Kinoshita, T., and Shimazaki, K. (2016). Plasma membrane H^+-ATPase1 (AHA1) plays a major role in *Arabidopsis thaliana* for stomatal opening in response to blue light. Plant Physiol. **171:** 2731–2743.

This information is current as of September 2, 2020

Supplemental Data	/content/suppl/2020/04/30/tpc.18.00802.DC1.html
References	This article cites 104 articles, 37 of which can be accessed free at: /content/32/7/2325.full.html#ref-list-1
Permissions	https://www.copyright.com/ccc/openurl.do?sid=pd_hw1532298X&issn=1532298X&WT.mc_id=pd_hw1532298X
eTOCs	Sign up for eTOCs at: http://www.plantcell.org/cgi/alerts/ctmain
CiteTrack Alerts	Sign up for CiteTrack Alerts at: http://www.plantcell.org/cgi/alerts/ctmain
Subscription Information	Subscription Information for *The Plant Cell* and *Plant Physiology* is available at: http://www.aspb.org/publications/subscriptions.cfm